

Biodegradable Foams

Original

Biodegradable Foams / Malucelli, Giulio (ACS SYMPOSIUM SERIES). - In: Polymeric Foams: Applications of Polymeric Foams (Volume 2) / Gupta R.. - ELETTRONICO. - Washington : ACS, 2023. - ISBN 9780841297166. - pp. 65-96
[10.1021/bk-2023-1440.ch004]

Availability:

This version is available at: 11583/2979268 since: 2023-06-08T17:09:25Z

Publisher:

ACS

Published

DOI:10.1021/bk-2023-1440.ch004

Terms of use:

This article is made available under terms and conditions as specified in the corresponding bibliographic description in the repository

Publisher copyright

ACS preprint/submitted version

(Article begins on next page)

Biodegradable foams

Giulio Malucelli

Dept. of Applied Science and Technology and local INSTM Unit, Politecnico di Torino,

Viale Teresa Michel 5, 15121, Alessandria Italy

E-mail: giulio.malucelli@polito.it

Biodegradable foams are currently gathering a wide interest from both academia and industry for several reasons, namely: resins from crude oil or natural gas are becoming less attractive since the price of the raw materials is incredibly increasing, hence stimulating the researchers toward the design and preparation of new products, which may represent a valuable alternative. Then, within the current circular economy concept, further attempts toward the reduction of wastes, and consequently, of their environmental impact, are being carried out, aiming at developing polymer resins from renewable sources, suitable for producing reliable polymeric foams. In this context, recyclability and/or biodegradability have become very important in modern society, in order to limit the landfill confinement of synthetic plastic wastes or products at the end of their life, also considering the significant growth of the world population and consequently the reduced available space for plastic confinement. These findings well justify the potentialities of these biodegradable polymers (and in particular of biodegradable foams) for different industrial applications.

This chapter aims at elucidating the materials, processes, and applications of biodegradable foams; finally, some perspectives about their possible further development in the next future are considered.

Introduction

Biodegradable foams are usually derived from natural/renewable sources and are biodegradable, i.e., they can degrade during time as a consequence of their interaction with the surrounding environment. In particular, biodegradation (also known as biotic degradation) is a chemical degradation process that some polymeric materials are able to undergo under specific conditions; it is activated by certain types of microorganisms, like fungi, bacteria, and algae.¹ It is necessary to discriminate between two different concepts, i.e., bio-based and biodegradable foams. The former, indeed, refer to the preparation and development of “bio”-foamed materials, usually deriving from the agro-food industry or other renewable fonts. A bio-based foam is undoubtedly bio-sourced, but it may not be biodegradable.

One of the most appropriate ways to generally define a biodegradable material is to consider it as a degradable product that undertakes the primary degradation through the action of microorganism metabolism, from which different degradation products originate. Therefore, biological activity is required. In this context, ASTM International has formulated an accurate definition of biodegradable material, as able to exploit the enzymatic action of specific microorganisms to decompose, giving rise to the formation of biomass, carbon dioxide, water, and methane. This decomposition, which must occur within a specified time interval replicating available disposal conditions, must be evaluated through standardized tests.²

For example, such natural polymer systems as nucleic acids, polysaccharides, and proteins usually degrade in (micro)biological environments through hydrolysis and oxidation reactions.³ As mentioned above, degradation leads to the formation of different products, according to the atmosphere, in which biodegradation occurs: in particular, during the aerobic biodegradation, the polymer gives rise to the formation of carbon dioxide, water, and biomass, leaving some residues comprising salts and minerals. Conversely, in anaerobic biodegradation, carbon dioxide is replaced by methane.^{4,5} Figure 1 schematizes the global carbon cycle: a substantial advantage in limiting the CO₂ emission is obtained from the use of biomass and bio-organics rather than crude oil-derived resources.

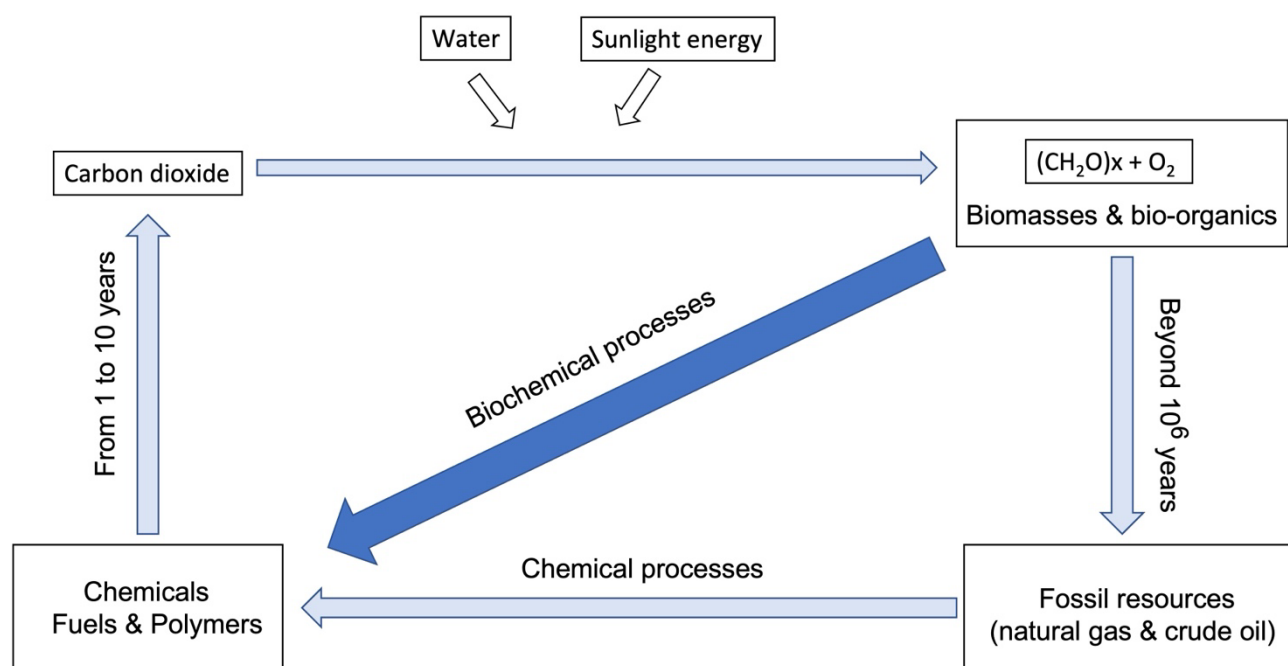


Figure 1: Scheme of the global carbon cycle

Generally speaking, polymeric materials (including foams) biodegrade according to three main consecutive steps:

- Biodeterioration: during this stage, the material is disintegrated into small fragments, through the action of abiotic sources (namely, moisture, UV radiation, oxygen/air, and environmental pollution, among others); the structure of the biodegrading polymer is almost preserved.
- Biofragmentation: it occurs when microorganisms produce free radicals and enzymes, which are able to convert the macromolecular chains into lower molecular weight products (i.e., oligomers and monomers).
- Assimilation/mineralization: in this final biodegradation step, the degrading products produced in the previous stage are first converted into metabolites, energy, and new biomass; then, during mineralization, the organic species are transformed into inorganic materials (such as salts) and gases (like CH_4 , CO_2 , and N_2).

Polymer biodegradability is significantly affected by several factors, namely: chemical structure (which determines the type(s) of functional groups and their stability/reactivity, the surface properties, and the swelling ability as well), molecular weight and molecular weight distribution, degree of crystallinity, porosity, and physico-mechanical behavior, among a few to mention.^{6,7}

Besides, a common classification of biodegradable polymers identifies 5 different types of materials, namely:

- Bio-degradable polymers, for which degradation takes place thanks to the action of naturally occurring micro-organisms comprising fungi, algae, and bacteria
- Bio-erodable polymers, which are oxidized, degraded, and eroded by weathering
- UV Bio-degradable polymers, broken by UV irradiation and further degraded
- Hydro Bio-degradable polymers, which undergo hydrolysis reactions and are further degraded
- Compostable polymers, which can be degraded into compost, giving rise to the formation of CO_2 , H_2O , biomass, and inorganic residues.

Table 1 collects the most important biodegradable polymers currently available on the market, together with their main applications. These biodegradable polymers can be processed in different shapes, hence giving rise to several final products, such as thin films (suitable for fabricating composting or shopping bags, landfill covers, and mulch films), or foams (as for packaging purposes, cups, trays, and service boxes).

In particular, biodegradable foams are gaining a lot of interest, not only from academics (as witnessed by the continuously increasing number of publications in peer-reviewed journals, Figure 2) but also from industries: indeed, apart from the “standard” characteristics that also may be referred to crude oil-derived non-biodegradable foams (including lightness, increased thermal insulation, dampening, sound absorption/insulation, and suitability for packaging purposes), some of the biodegradable foams (such as those based on ethylene vinyl alcohol or polyvinyl alcohol) are water-soluble, hence limiting the environmental impact in both their managing and final disposal. Besides, the landfill

confinement of biodegradable foams may favor the degradation of the landfill wastes, hence lowering the landfill space utilization.

Table 1: Main commercially available biodegradable polymers

Polymer	Usual processed shape	Application sectors
Polyvinyl alcohol	Foams or Films (water-soluble)	Packaging
Polycaprolactone	Foams or Films	Packaging
Starch (including starch-based blends)	Loose-fill Foams	Packaging
Ethylene vinyl alcohol	Foams or Films (water-soluble)	Packaging
Polylactic acid and biodegradable polyesters	Sheets	Thermoformable sheets

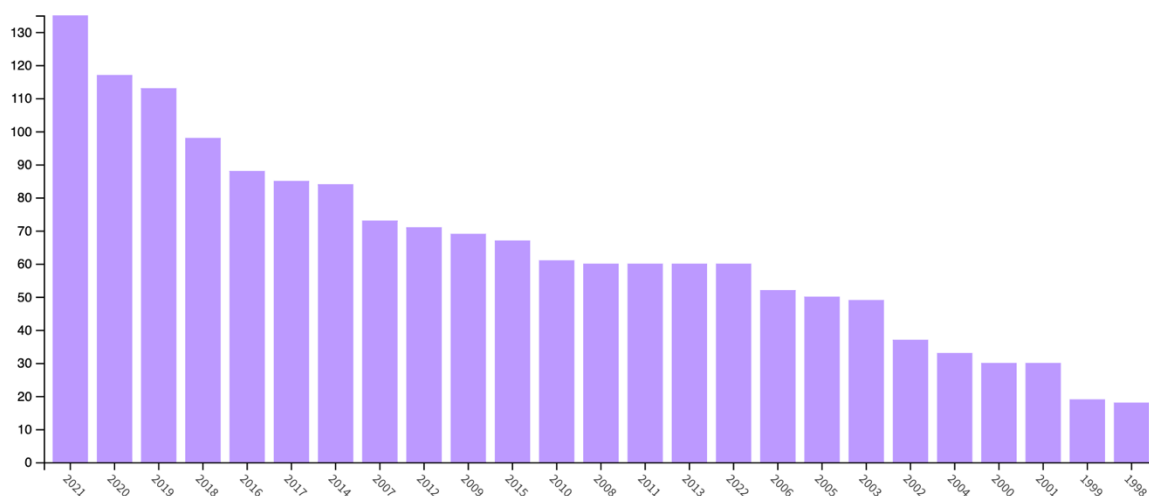


Figure 2: Number of publications (from 1998 to 2021) in peer-reviewed journals, dealing with biodegradable foams (From Web of ScienceTM database, accessed on 5 July 2022).

From a historical point of view, the development of biodegradable foams dates back to the mid of 1960s, when Proznán and co-workers succeed in extruding starch to obtain a “foamed” gelatinized material; from that point onwards, there has been a rapid development, as evidenced by the huge number of filed patents (Table 2).

Table 2: Patent developments on biodegradable foamed materials

Patent Year	Patent number	Inventors	Patent topic
1964	US 3,137,592	Protzman, Wagoner	Extrusion of starch to produce a foamed product
1975	US 3,891,624	Boonstra, Berkhout	Extrusion of hydrophobic porous starch
1989	US 4,863,655	Lacourse, Altieri	Biodegradable packaging made of starch foam
1991	US 5,035,930	Lacourse, Altieri	Biodegradable shaped products
1992	US 5,089,535	Malwitz, Lee	Water-soluble polyvinyl alcohol foams
1996	US 5,554,660	Altieri, Tessler	Starch foam with enhanced water/humidity resistance
1996	US 5,506,277	Griesbach	Starch foams for absorbent articles
1998	US 5,766,749	Kakinoki, Sato	Biodegradable foam material
1998	WO 9851466	Schennink	Biodegradable foam moldings made of thermoplastic starch

2001	WO 0160898	Bastioli, Lombi, Salvati	Foamed starch sheets
2002	WO 0220238	Van Tuil, Van Heemst	Foamed biopolymer-based products and process of producing
2002	US 6,406,649	Fisk	Biodegradable foamed starch product
2004	US 6,740,731	Bigg, Sinclair, Lipinsky, Litchfield, Allen	Disposable materials from hydroxycarboxylic acid copolymer (comprising foamed products)

The present chapter aims at providing the reader with a short comprehensive overview of the materials used to produce biodegradable foams, the related processes employed, and some applications of the obtained products. Finally, some recent outcomes from the scientific literature will be presented, together with some outlooks about the possible further development of biodegradable foamed materials in the forthcoming years.

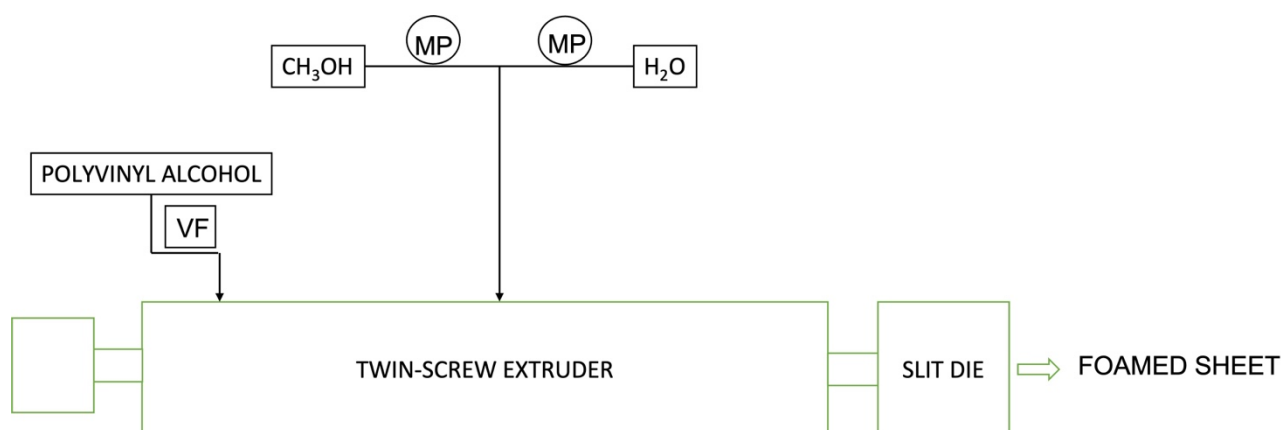
Types of biodegradable foams and foaming technologies: a general overview

Several different types of biodegradable foamed products have been designed and developed during the last decades. The next paragraphs will classify the biodegradable foams on the basis of their chemical structure, elucidating the production processes and their main characteristics: in particular, the classification will involve three main biodegradable foams, namely polyvinyl alcohol-, starch-, and polylactic acid-based foams. Polyurethane foams, which may also biodegrade, are biodegradable mainly for the polyol-derived structures present in the polymer network and are produced using the standard processes already available for polyurethanes: they will be discussed later, in a specific paragraph related to some recent advances.

Polyvinyl alcohol-based biodegradable foams

Polyvinyl alcohol is a thermoplastic, water-soluble and biodegradable copolymer, derived from the hydrolysis of polyvinyl esters, such as polyvinyl acetate; usually, extrusion processes are exploitable for obtaining foamed materials. Foaming can be performed by extrusion, using methanol and water as foaming agents, as schematized in Figure 3. Though the foaming process is well established, it has to be considered that the polymer has a great propensity to start decomposing before melting: therefore, the foaming extrusion process has to be performed on a stable polyvinyl alcohol melt.⁸

The presence of pendant OH groups on alternating carbon atoms in the skeleton of the copolymer accounts for the occurrence of high intra- and inter-molecular hydrogen bonding, which, in turn, influences the solubility in water of the copolymer, its glass transition temperature, and the overall mechanical behavior as well. Therefore, it is very important to limit hydrogen bonding interactions in order to be able to perform foaming extrusion processes. Besides, the melting temperature of polyvinyl alcohol strictly depends on the hydrolysis degree of the copolymer, its molecular weight and molecular weight distribution, as well as the possible presence of plasticizers (such as glycerol, PEG, and neopentyl glycol).



VF: Volumetric Feeder

MP: Metering Pumps

Figure 3: Scheme of the foaming extrusion process of polyvinyl alcohol

Starch-based biodegradable foams

Starch is a polysaccharide that can be extracted from several tubers, seeds, pollen, roots, and fruits in a wide variety of granular shapes, such as platelets, spheres, irregular tubules, and ellipsoids (average shape size between 0.5 and 175 μm). The structure of starch comprises repeating units of glucose linked by glycoside bonds. Two main macromolecules can be identified in the polysaccharide, namely amylose, which represents the flexible linear fraction, and amylopectin, which is the most abundant and highly branched fraction.⁹ In particular, during the foaming process, amylopectin provides suitable foamability and melt strength, while amylose ensures flexibility.

The starch family comprises various types of polysaccharides, namely potato starch, tapioca starch, corn starch (also pregelatinized), native starch, and modified starch (i.e., hydroxy-ethylated or hydroxy-propylated starch); their price is quite variable.

In order to produce foamed products (Figure 4), starch can undergo two different methods. The first (similar to that shown in Figure 3 for polyvinyl alcohol) employs an extruder (usually a twin-screw apparatus, though single-screw extruders can be utilized as well): starch is heated up in the extruder until melting, subsequently mixed with water and methanol (usually exploited as blowing agents), and finally forced to pass through a die for expansion to occur. During this last step, pressure drops down, hence favoring the water vapor diffusion into nucleated bubbles and, therefore, the foaming of the polysaccharide. Different experimental parameters affect the density of the obtained foam, i.e., the foaming process: some of them refer to the employed starch (type, molecular weight, molecular weight distribution, moisture content), some others to the twin-screw configuration (elements of the screw, temperature profile of the barrel), and to the possible presence of nucleating agents and additives. Two different limiting issues have to be taken into account, in order to optimize the foaming process and to obtain starch foams suitable for different uses, namely corrugation (that has to be suppressed) and the percentage of closed cells (that has to be increased as much as possible). The second method that can be exploited for obtaining foamed molded components is pellet expansion: in this case, starch pellets are immersed into a fluid that has a low boiling point and then put in a closed mold and heated up very rapidly.

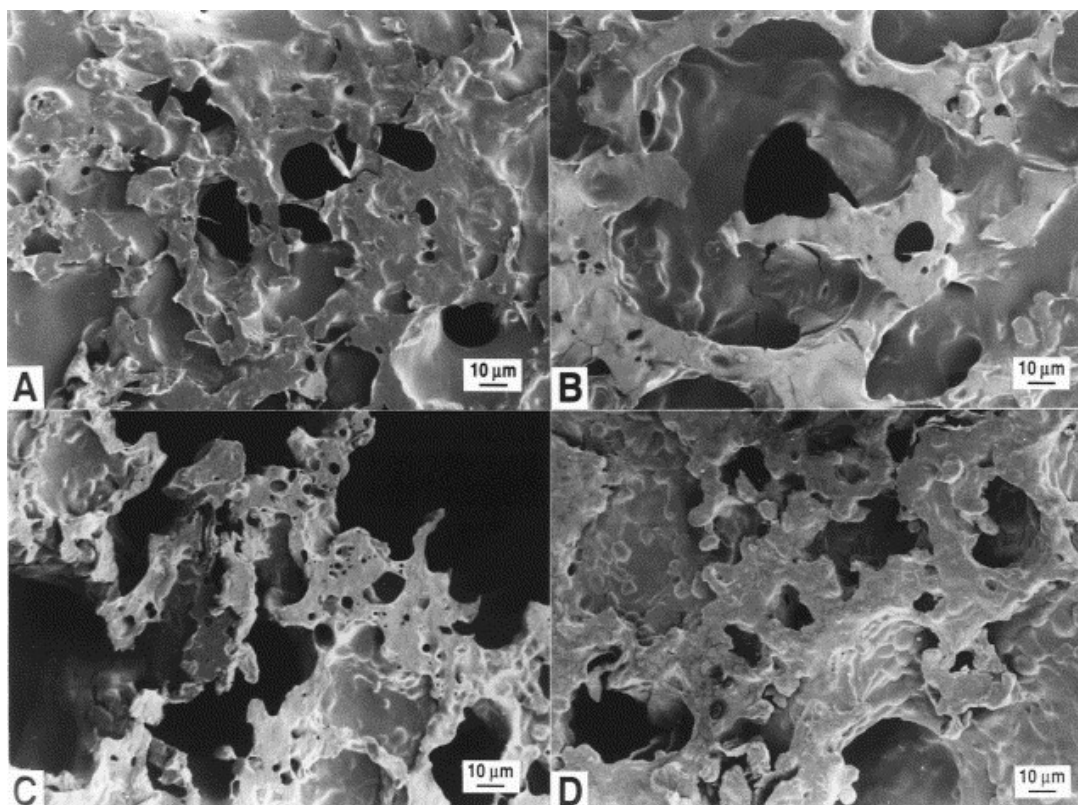


Figure 4: Scanning electron micrographs of surfaces of baked foam plates made from waxy maize starch (A), normal corn starch (B), high (50 wt.%) amylose corn starch (C), and high (70 wt.%) amylose corn starch (D). Reprinted with permission from reference 10. Copyright (1998), Elsevier.

The flexibility and impact resistance of the obtained foamed products can be adjusted quite properly by selecting the specific type of starch (i.e., increasing the amylose to amylopectin ratio) and/or by incorporating some chemical additives (such as glycerol, polyethylene glycol, sorbitol, among a few to mention), which may act as plasticizers. However, conditioning the foam at very low relative humidity for extended times may determine a significant embrittlement of the material, even in the presence of the aforementioned plasticizers or by using high amylose/amylopectin ratios.

If compared with EPS (expanded polystyrene), the bulk density of foamed starch is on average two times higher than that of the former (Table 3): this is due to the fact that (i) the density of polystyrene is 30% less than starch, and therefore, to have a comparable density after foaming, the efficiency of the foaming process of starch should be significantly higher with respect to that achievable in the standard foaming plants, and (ii) starch cells are bigger, more open and less regular with respect to polystyrene cells.¹⁰

Table 3: Comparison between expanded polystyrene and foamed starch

	Expanded Polystyrene	Starch Foam
Price (\$/kg) (2022)	0.70-0.90	1.90-2.50
Cell Geometry	Pentagonal (regular)	Irregular
Cell size (mm)	0.15-0.35	0.60-0.80
Type of cells	Closed cells	More open cells
Bulk density (kg/m ³)	4.2	9.6
Moisture sensitivity	Low	High
Melt Strength	Quite poor	High
Foaming processing window	Wide	Narrow

Polylactic acid (poly (3,6-dimethyl-1,4-dioxane-2,5-dione, PLA) is a semi-crystalline aliphatic biodegradable and compostable polyester (as certified by DIN CERTCO (DIN 54900-1, DIN 54900-2, and DIN 54900-3)), which derives from lactic acid, i.e., the fermentation product of such natural sugars as glucose originating from the hydrolysis of starch. PLA can be obtained by means of polycondensation reactions of the monomer, or by ring opening of lactides (namely, L-lactide, D-lactide, and meso-Lactide), i.e., dimers of lactic acid. Among these dimers, meso-lactide melts at lower temperatures with respect to the other two dimers; besides, the content of D- and meso-lactides in polylactic acid macromolecular chains remarkably affects the thermal behavior, i.e., the melting and crystallization temperatures, and rate of crystallization as well. As an example, both rates of crystallization and melting temperatures decrease when increasing amounts of D-lactide are incorporated into the polymer. In particular, limiting the D-lactide content in the polymer accounts for obtaining PLA products with high degrees of crystallinity and acceptable dimensional stability up to 140°C; conversely, the dimensional stability can be significantly reduced below 45°C when high D-lactide amounts are present, giving rise to the formation of totally amorphous products. Obviously, all these findings may considerably affect the overall processability of PLA and even its foaming processes. These latter are usually performed by means of a twin-screw extruder; the overall process involves three main steps, i.e., the actual extrusion, the stabilization, and the final winding. With respect to foaming processes applied to other foamable polymers, since polylactic acid is very sensitive to moisture, it necessitates drying before being fed to the extruder. Usually, the pre-dried polymer is mixed with talc (acting as a nucleating agent) and other processing aids that enhance the foaming and cell creation. Hydrocarbons, CO₂, or hydrochlorofluorocarbons (HCFCs) can be employed as effective foaming agents for PLA. During foaming extrusion, it becomes very important to reduce the shear stresses and to boost the cooling, because of the quite low glass transition temperature (usually between 50 and 80°C) of the polymer.

Recent advances in biodegradable foams

The next paragraphs will discuss and summarize some of the most recent achievements in the design, synthesis, and processing of biodegradable foams, providing the reader with an overview of the current progress and still challenging issues.

Progresses in biodegradable polyurethane foams

Some current research on biodegradable foam deals with the modification of polyurethane foams with functional additives or fillers able to tune the degradability of the foam. In this context, Yu and co-workers¹¹ employed bagasse (an agricultural waste very abundant in the south of China, bearing several hydroxyl groups) and a soy oil-based polyol as raw components for the formulation of biodegradable polyurethane foams, using polymeric methylene diphenyl diisocyanate as co-reactant; distilled water was utilized as the foaming agent. The bagasse content in the polyurethane formulation was changed from 2.5 to 12.5 wt.%. The concurrent presence of the two components turned out to remarkably increase the biodegradation of the foam, as assessed through the ASTM D5988 standard (soil burial method): in particular, a reaction between the bagasse and the polymeric diisocyanate was hypothesized, which accounted for the incorporation of an easily degradable segment into the polyurethane foam, hence improving the biodegradability with respect to a similar polyurethane foam not containing the bagasse and made with a crude oil-derived polyol.

Using a similar approach, Paciorek-Sadowska and co-workers¹² investigated the effect of two polyols, namely a polyetherol based on metasilicic acid and the product obtained from the glycolysis of polylactic acid waste on the biodegradability, thermal properties, and flame retardance of rigid polyurethane foams. Figures 5 and 6 schematize the synthesis of the two polyols.

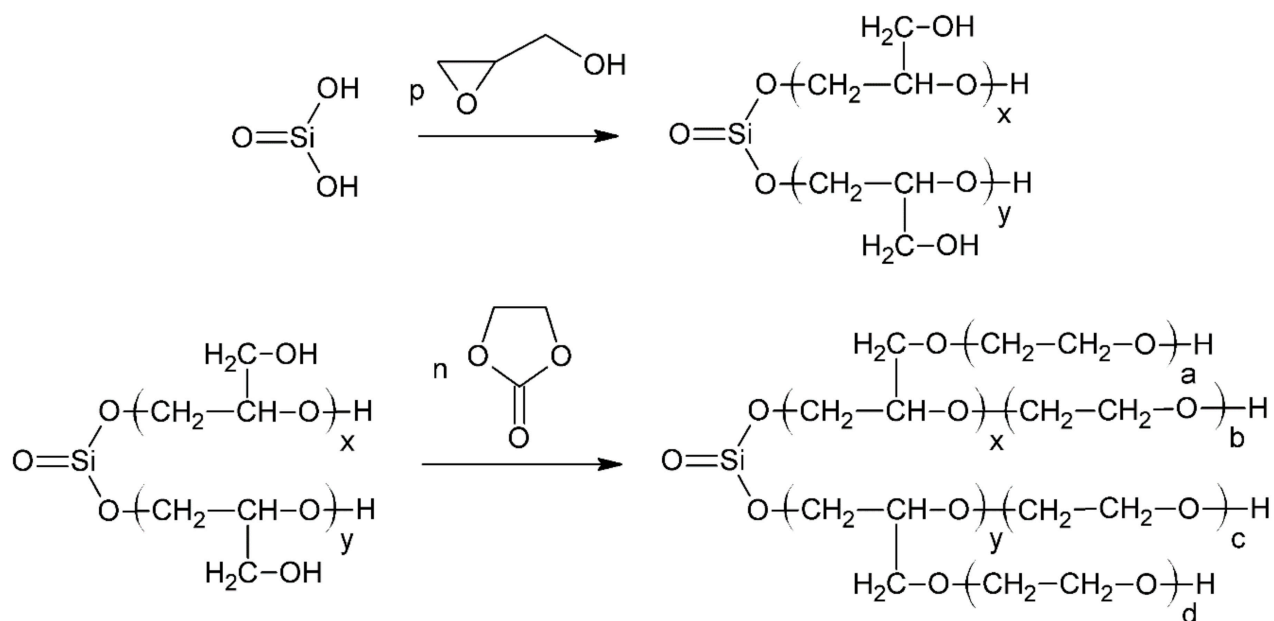


Figure 5: Scheme of synthesis of the polyol based on metasilicic acid (where: $p = x + y$ and $n = xa + b + c + yd$). Reprinted from reference 12 under CC BY license.

Among the polyurethane formulations, that containing 50% of each polyol was compared with the polymer made of 100% of the polyetherol based on metasilicic acid, chosen as a reference.

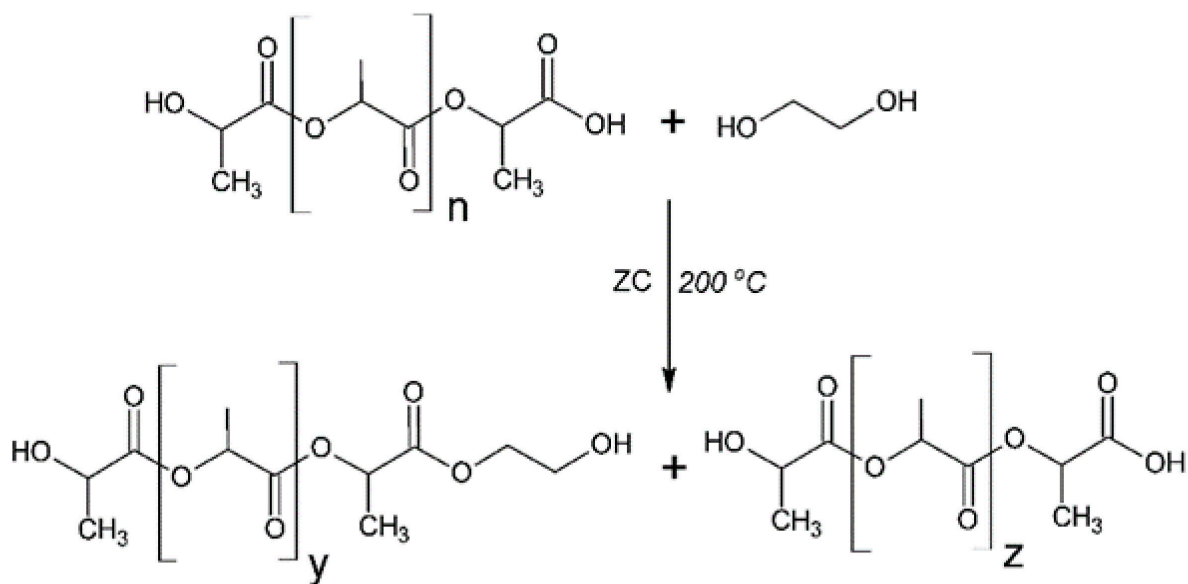


Figure 6: Scheme of synthesis of the polyol derived from the glycolysis of polylactic acid waste (where $n = y + z$; ZC: zinc stearate, used as a catalyst). Reprinted from reference 12 under CC BY license.

The biodegradability of the prepared foams was assessed by means of a respirometric method (according to the ISO 17556:2019 standard), evaluating the oxygen demand needed for aerobic biodegradation of the polyurethanes in soil. Table 4 collects the biochemical oxygen demand (BOD) after 28 days, the theoretical oxygen demand (TOD), based on the elemental analysis of the foams, which is needed for biodegradation, and the resulting degree of biodegradation: it is clear that, unlike the polyurethane foam made with 100% of the polyetherol based on metasilicic acid, which did not biodegrade, the counterpart containing both the polyols showed a high degree of biodegradation (equal to 68.4%).

Table 4: Comparison between BOD at 28 days, theoretical oxygen demand (TOD), and degree of biodegradation for the two polyurethane foams investigated

Type of polyurethane foam	BOD ₂₈ (mg/l)	TOD (mg/l)	Degree of biodegradation (%)
Containing 100% of polyetherol based on metasilicic acid	0	73.6	0
Containing 50% of the two polyols	54.9	80.3	68.4

Besides, the presence of Silicon in both the foam formulations accounted for a significant decrease in the flammability and increase in the thermal resistance: in particular, the foam containing both the polyols was able to withstand long-term exposures to temperatures as high as 175°C; in addition, this foam exhibited decreased apparent density (from 96 – for the reference foam - to 89 kg/m³) and thermal conductivity (equal to 0.034 W/(mK), with respect to 0.037 W/(mK) of the reference material).

In a further research effort, Fang and co-workers¹³ exploited a continuous microflow system for obtaining new polyols derived from the ring opening reaction between epoxidized soybean oil (obtained through epoxidation of soybean oil) and a polyhydroxy compound (synthesized by reacting glycerol with styrene oxide); the obtained polyols were employed for preparing biodegradable rigid polyurethane foams; a schematic of the overall process is depicted in Figure 7; Figure 8 shows the reactions involved. For comparing purposes, a rigid polyurethane foam was also prepared using a batch process: regardless of the employed process (i.e., continuous or batch), the polyurethane foams showed a closed-cell structure (Figure 9): however, the cell size of the foams obtained through the continuous microflow system was more regular (hexagon-like), uniform, and complete with respect to that resulting from the batch process. In addition, the continuous microflow system allowed obtaining foams with higher specific compression strength as compared to the batch process. Finally, biodegradability was claimed by the authors, although no biodegradability tests were carried out.

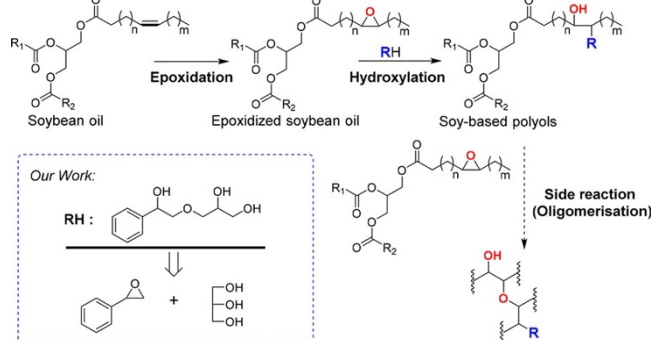


Figure 7: Synthetic path for the preparation of soy-based polyols. Reprinted with permission from reference 13. Copyright (2019), American Chemical Society.

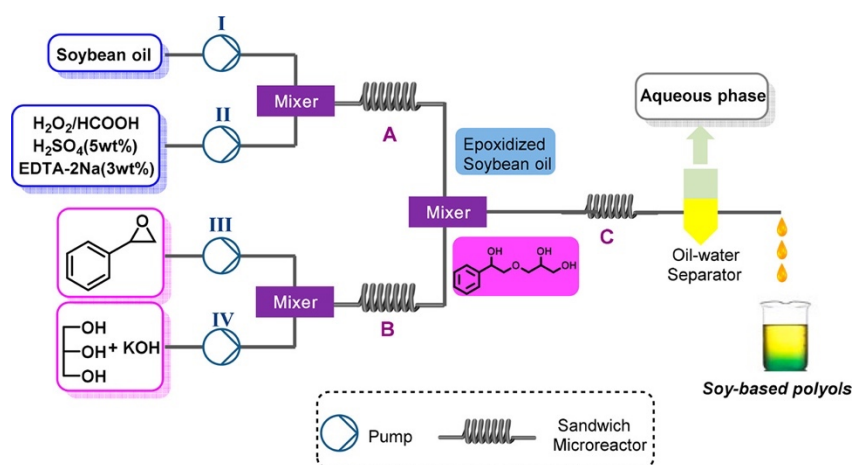


Figure 8: Scheme of the synthesis of soy-based polyols. Reprinted with permission from reference 13. Copyright (2019), American Chemical Society.

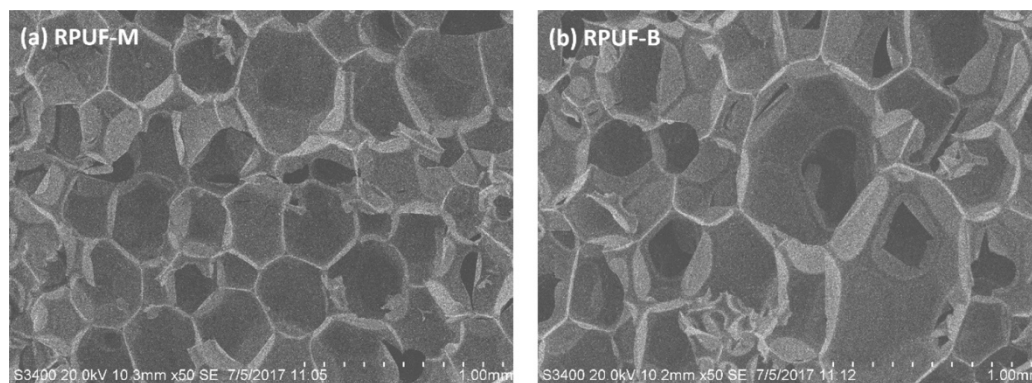


Figure 9: Typical SEM images of the rigid polyurethane foams prepared by means of continuous flow system ((a) RPUF-M) and batch ((b) RPUF-B) processes. Reprinted with permission from reference 13. Copyright (2019), American Chemical Society.

Luo and co-workers¹⁴ designed biodegradable self-foaming rigid polyurethane foams through a one-pot reaction between polymeric methyldiphenyl diisocyanate and all bioresource-based polyols (derived from lignin powder and soybean phosphate ester polyol). Different lignin powder loadings (namely, 5, 10, 15, 20, and 25 wt.% of the total polyols content) were employed. As assessed by FT-IR spectroscopy, the obtained foams showed the appearance of -C=O signals at 1705 cm^{-1} , attributed to the formation of hydrogen bonds between the lignin polyols and the urethane groups of soy polyol-based polyurethane segments. Further, increasing the lignin content in the polyurethane formulation accounted for a significant improvement in the mechanical behavior, as shown in Figure 10 for the specific compression modulus.

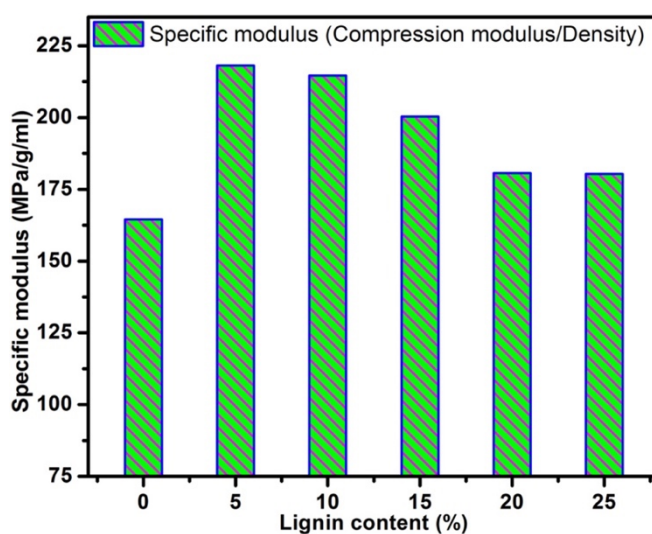


Figure 10: Typical SEM images of the rigid polyurethane foams prepared by means of continuous flow system ((a) RPUF-M) and batch ((b) RPUF-B) processes. Reprinted with permission from reference 14. Copyright (2018), Elsevier.

Finally, biodegradability was assessed through soil burial tests¹⁵ (soil pH=7) carried out for 16 weeks. As shown in Figure 11, the weight loss was below 10% within the test duration, regardless of the polyurethane foam composition. Besides, it is worthy to highlight that the presence of increasing amounts of lignin in the foam formulation accounted for an overall increase in its biodegradation propensity. This finding was attributed to the high polar character of the lignin, which favored the water absorption, hence improving the degradation level of the foam.

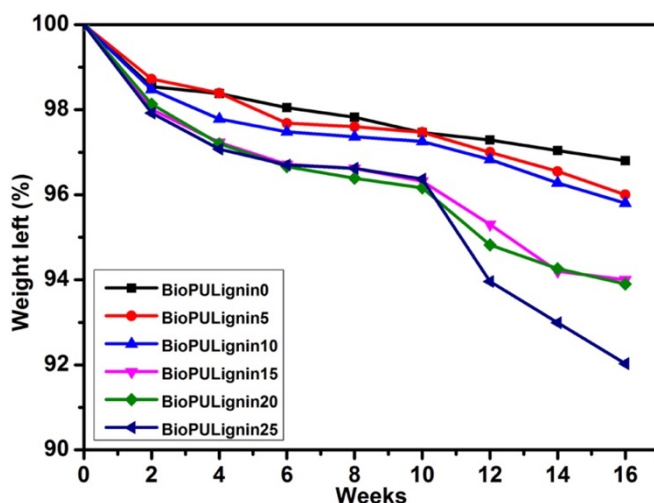


Figure 11: Results of soil burial tests (in terms of weight loss vs. time) for rigid polyurethane foams containing different lignin loadings (BioPULigninX, where X is the lignin wt.% loading). Reprinted with permission from reference 14. Copyright (2018), Elsevier.

Then, white mustard seed oil and 2,2'-thiodiethanol were exploited for the design and obtainment of biodegradable rigid polyurethane/polyisocyanurate foams.¹⁶ In particular, a petrochemical polyol (namely, Rokopol RF-551, derived from oxyalkylation of sorbitol) was partially replaced with increasing amounts of the synthesized bio-polyol (up to 0.4 chemical equivalent of hydroxyl groups every 0.1 equivalent (Eq.) of petrochemical polyol). The resulting mixtures were reacted with Purocyn B, a technical polyisocyanate containing 4,4'-diphenylmethane diisocyanate as the main component. A mixture of 1,1,1,3,3-pentafluorobutane and 1,1,1,2,3,3,3-heptafluoropropane (87:13 mass ratio) was utilized as foaming agent; further, tri(chloro-2-methylethyl) phosphate was incorporated in half of the synthesized polyurethane systems, as flame retardant additive.

After the foaming process, the incorporation of increasing amounts of the bio-polyol in the foam formulation gave rise to the formation of closed cells with larger diameters and with slightly higher wall thicknesses as compared to the material containing 100% of the petrochemical polyol (Figure 12).

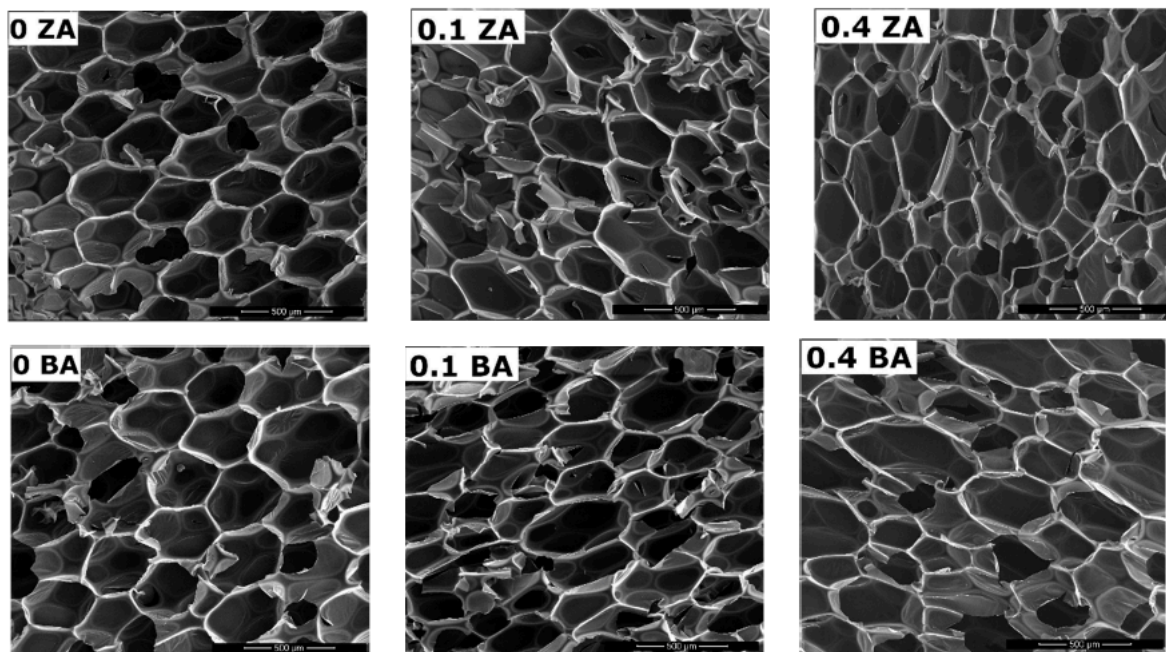


Figure 12: SEM micrographs of cellular structure of rigid polyurethane/polyisocyanurate foams with 0, 0.1, and 0.4 Equivalent of bio-polyol (ZA= flame retarded foams; BA= foams without the flame retardant additive). Reprinted from reference 16 under CC BY license.

The presence of increasing amounts of bio-polyol affected the overall mechanical behavior of the foams, as shown in Figure 13: more specifically, the partial replacement of the petrochemical polyol with the bio counterpart slightly worsened the compressive strength and the apparent density values as well, though they were still acceptable as compared to commercially available rigid polyurethane foams. The observed trend was ascribed to the presence of increasing amounts of the bio-polyol, bearing long linear chains, which decreased the degree of macromolecular packing in the obtained foams.

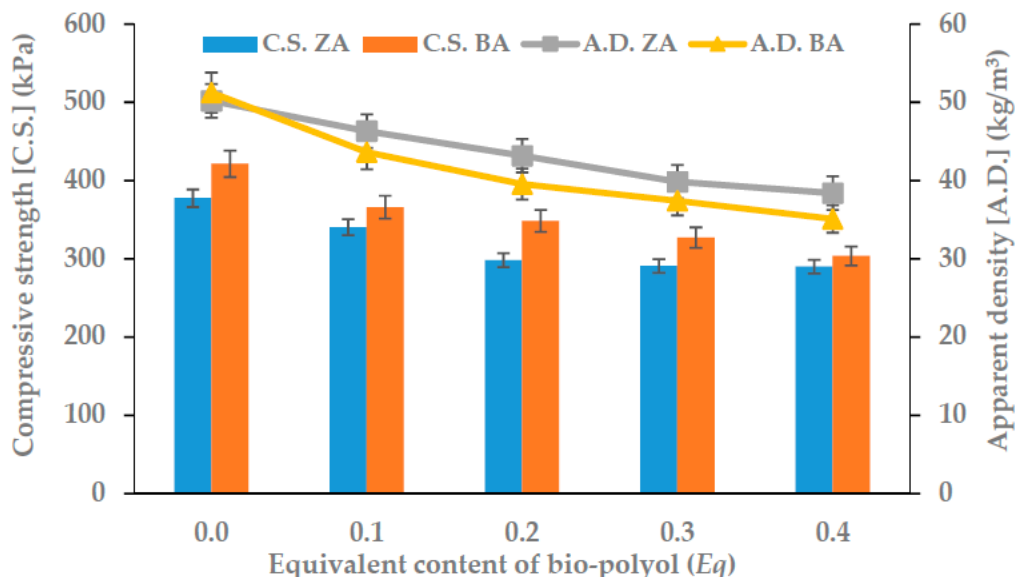


Figure 13: Compressive strength (C.S.), and apparent density (A.D.) of the synthesized rigid polyurethane/polyisocyanurate foams as a function of the bio-polyol content (ZA= flame retarded foams; BA= foams without the flame retardant additive). Reprinted from reference 16 under CC BY license.

Conversely, the observed lowering in the degree of macromolecular packing with increasing the bio-polyol content accounted for a significant increase in the foam toughness, as shown in Figure 13.

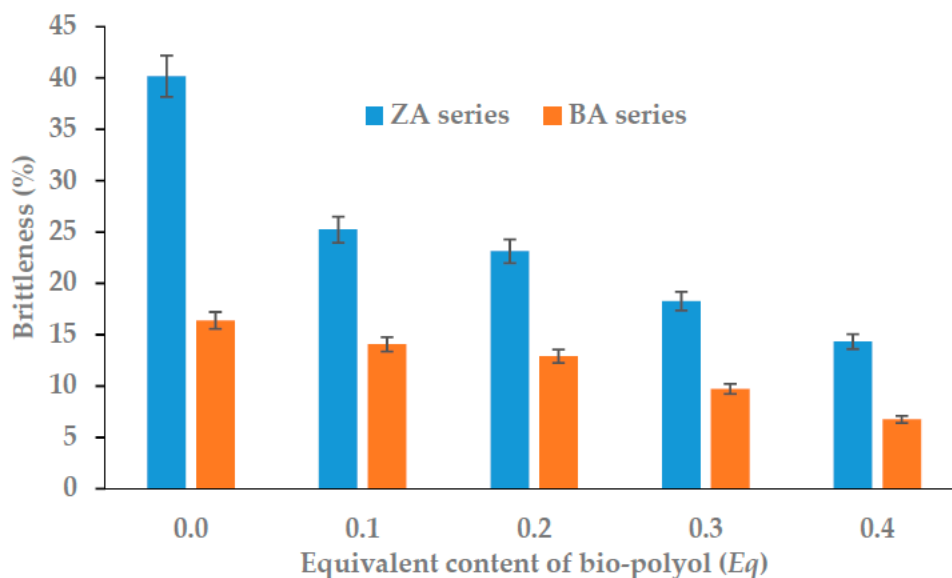


Figure 14: Brittleness of the synthesized rigid polyurethane/polyisocyanurate foams as a function of the bio-polyol content (ZA= flame retarded foams; BA= foams without the flame retardant additive). Reprinted from reference 16 under CC BY license.

The biodegradability of the prepared foams was assessed by means of a respirometric method (according to the ISO 17556:2019 standard), evaluating the oxygen demand needed for aerobic biodegradation of the materials in soil. Table 5 collects the biochemical oxygen demand (BOD) after 28 days, the theoretical oxygen demand (TOD), based on the elemental analysis of the foams, which is needed for biodegradation, and the resulting degree of biodegradation. It is worth noticing that, unlike the polyurethane/polyisocyanurate foams made with 100% of the petrochemical polyol, which showed limited biodegradation in soil, the counterpart containing both the bio-polyol significantly increased the propensity to biodegrade. This finding was attributed to the presence of Sulphur in the bio-polyol formulation, which favors the development of the micro-organisms present in the soil ¹⁷, hence increasing the degree of biodegradation.

Table 4: Comparison between BOD at 28 days, theoretical oxygen demand (TOD), and degree of biodegradation for the foams investigated

Type of polyurethane foam	BOD ₂₈ (mg/l)	TOD (mg/l)	Degree of biodegradation (%)
Foam with 100% petrochemical polyol	7.1	90.3	7.9
Foam with 0.4 Eq. of bio-polyol	38.0	97.5	39.0
Flame retarded foam with 100% petrochemical polyol	7.0	87.2	8.0
Flame retarded foam with 0.4 Eq. of bio-polyol	70.4	95.0	74.1

Finally, as assessed by horizontal flame spread tests, all the foams containing the flame retardant, as well as the formulation with the highest content of the bio-polyol (i.e., 0.4 Eq.), but not containing the flame retardant additive, achieved self-extinction.

A practical application of biodegradable foams comes from the recent work of Mukherjee and co-workers ¹⁸, who synthesized a biodegradable flexible polyurethane foam suitable as a shoe insole. To this aim, polycaprolactone triol was employed as polyol, together with 1,4-butanediol (as chain extender); the mixtures were reacted with 1,6-diisocyanato-hexane, in the presence of the blowing agents (hexane and bis-2-dimethylamine ethyl ether). A general scheme is presented in Figure 15.

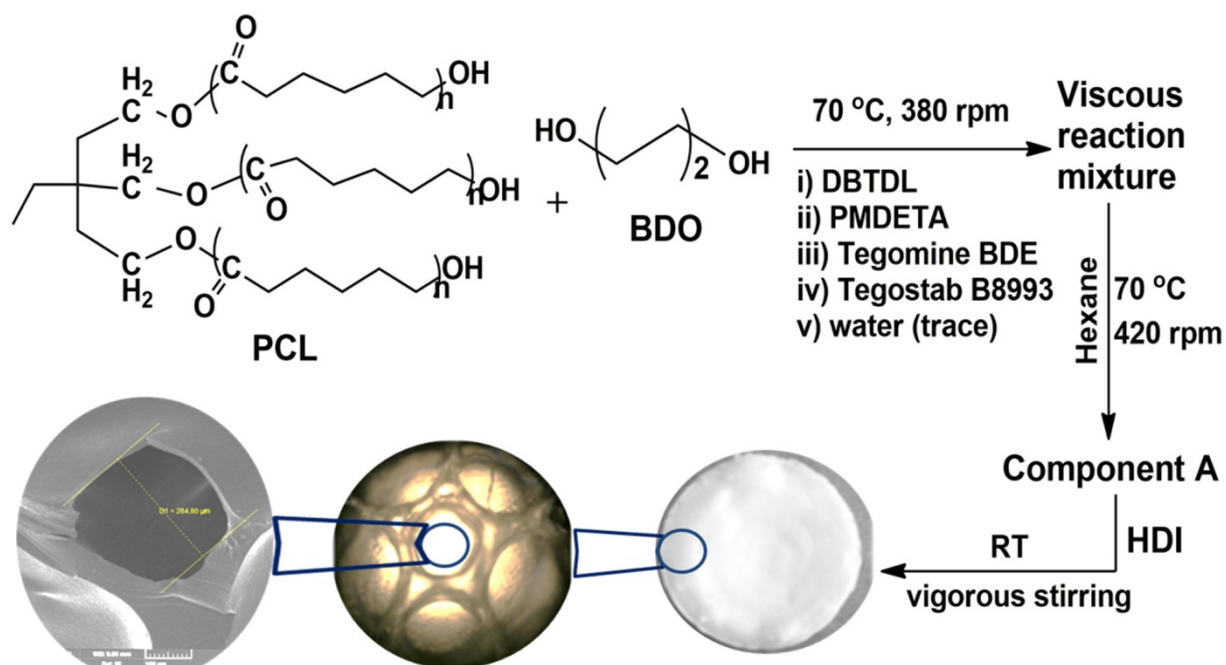


Figure 15: Scheme of the preparation of the polyurethane foams. Legend: PCL=polycaprolactone triol; BDO=1,4-butanediol; DBTDL=dibutyltin dilaurate; PMDETA=N,N,N',N',N''-pentamethyl diethylenetriamine; HDI=1,6-diisocyanato-hexane; Tegomine BDE=bis-2-dimethylamine ethyl ether; Tegostab B8993=polyether-polydimethyl siloxane copolymer; RT=room temperature. Reprinted with permission from reference 18. Copyright (2020), Elsevier.

As also assessed by different mechanical tests, the optimized polyurethane foam formulations turned out to be suitable for the shoe insole application; besides, the authors claimed the biodegradability of the prepared foams, though no biodegradability test was carried out.

Progresses in polylactic acid-based biodegradable foams

Very recently, Li and co-workers¹⁹ designed and produced biodegradable polylactic acid/polybutylene succinate (PLA/PBS) foams with remarkable selectivity toward oil adsorption. In particular, polylactic acid was employed as the matrix of the new foams, while polybutylene succinate for opening the cells; further, the foaming process exploited supercritical carbon dioxide. First, as shown in Figure 16, polylactic acid/polybutylene succinate blends with different PBS loadings (namely, 0, 10, 20, 30, 40, and 50 wt.%) were prepared in a twin-screw extruder; subsequently, the blends were employed in the foaming process, using different experimental conditions (i.e., saturation pressure, foaming temperature, and depressurization rate).

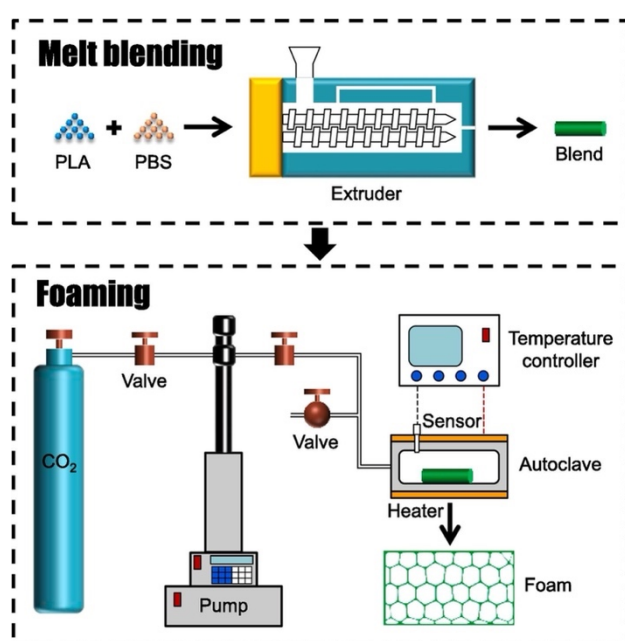


Figure 16: Scheme of the preparation process of the polylactic acid/polybutylene succinate foams. Reprinted with permission from reference 19. Copyright (2021), Elsevier.

The cell morphology of some typical PLA/PBS foams is presented in Figure 17 as a function of the foaming temperature: it is noteworthy that when the foaming process was carried out at 115°C, all the foams showed an amorphous uniform cell morphology (cell size between 100 and 300 µm). Lowering the foaming temperature to 105°C accounted for the appearance of crystalline structures (i.e., spherulites, with size between 50 and 100 µm), giving rise to the formation of flower-like morphologies surrounded by the foam cells (see the red circles in Figure 17), irrespective of the composition of the foam. Besides, when the foaming process was performed at 115°C, all the blends but neat PLA (i.e., PLA/PBS0 sample, which exhibited a closed-cell morphology) showed an open-cell morphology, which gradually increased with increasing the PBS loading.

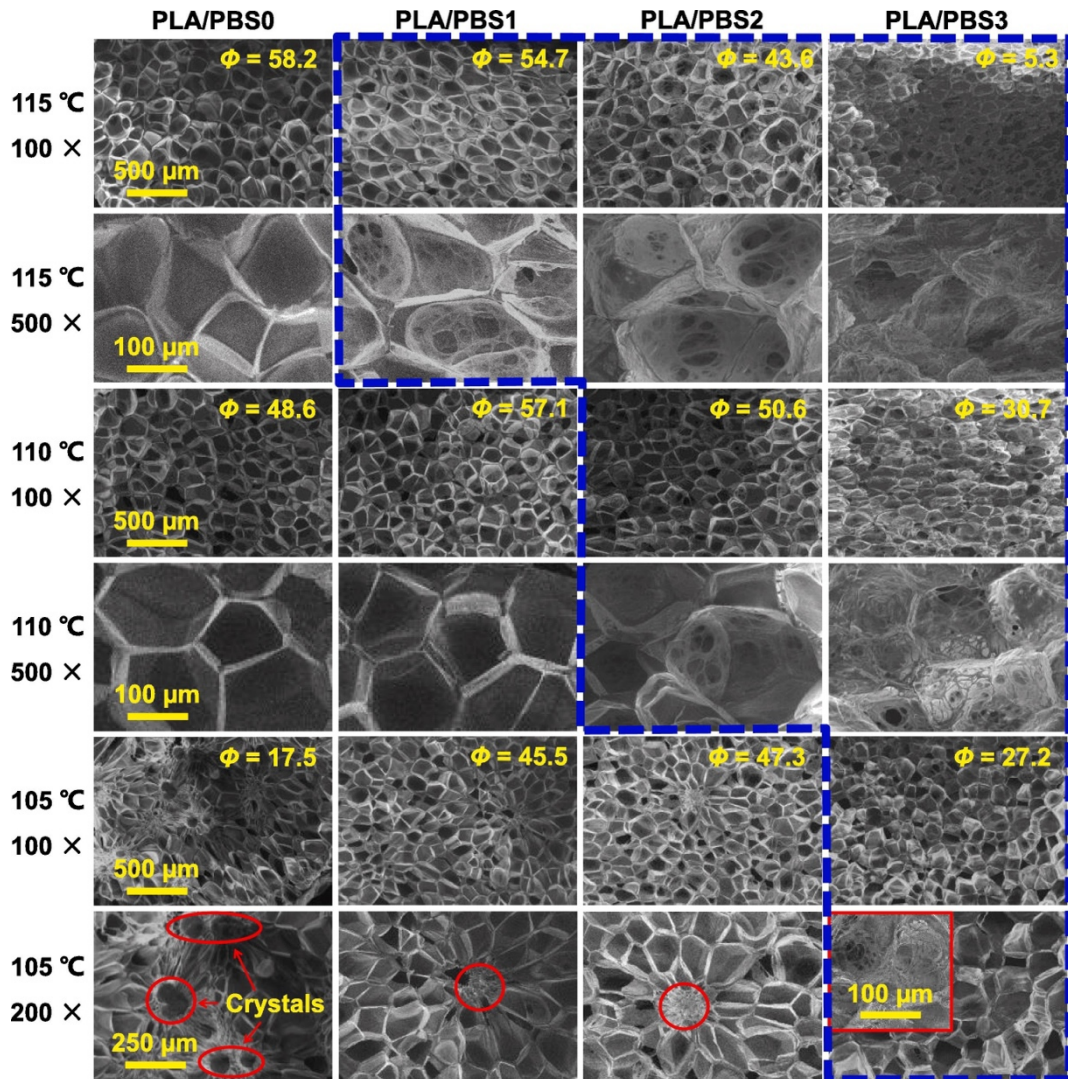


Figure 17: SEM pictures showing the cell morphology of foams containing different polybutylene succinate loadings and prepared at various foaming temperatures. Legend: PLA/PBSx indicates the composition of the prepared foam, where X denotes the PBS loading; 0: no PBS, 1: 10 wt.% of PBS, 2: 20 wt.% of PBS, 3: 30 wt.% of PBS. ϕ is the expansion ratio, i.e., the ratio of the density of the solid to that of the foamed material. Reprinted with permission from reference 19. Copyright (2021), Elsevier.

As shown in Figure 18, the foamed polylactic acid/polybutylene succinate blends exhibited a selective absorption of oil from water. Finally, the authors claimed the biodegradability of the foamed blends, though no biodegradability test was carried out.

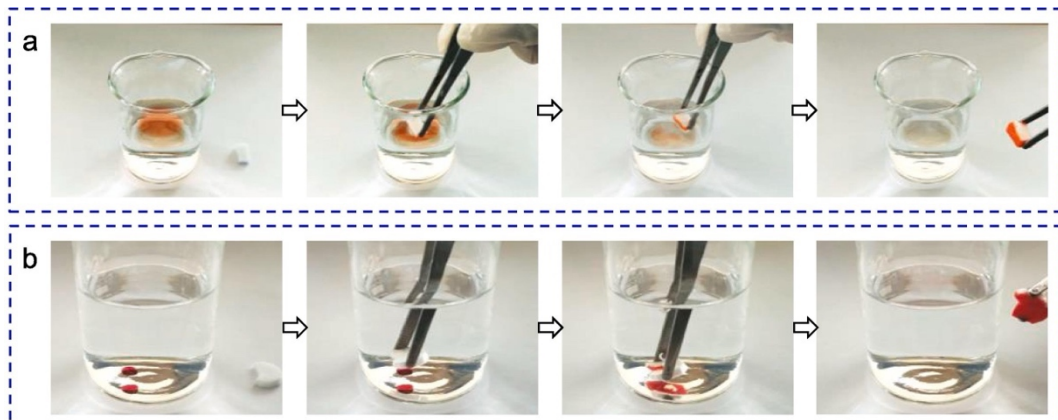


Figure 18: Removal process of Sudan Red dyed (a) cyclohexane and (b) CCl_4 from water by the foam containing 20 wt.% of PBS. Reprinted with permission from reference 19. Copyright (2021), Elsevier.

The current research on biodegradable polylactic acid-based foams has also been addressed toward the investigation of nanostructured systems. In this context, Borkotoky and co-workers²⁰ prepared biodegradable polylactic acid/cellulose nanocrystals (PLA/CNC) foams, exploiting a casting and leaching technique for the obtainment of highly porous morphologies (average porosity: about 81%). To this aim, fine sucrose particles were embedded into PLA, together with cellulose nanocrystals (at three different loadings, namely 1, 2, and 3 wt.%); then, after casting, the sucrose particles were easily removed with water, hence giving rise to the formation of the foamed structures. As assessed by FESEM (Figure 19), all the prepared foams, irrespective of the CNC loading, exhibited the formation of open-cell interconnected structures, with a peculiar surface texture that was responsible for the highly hydrophobic character of the foams. In fact, the as-prepared foams showed high static contact angle values with water (about 127°), unlike the foams that underwent a compression stage, hence gathering a smoother surface and lower hydrophobicity.

Finally, the authors claimed the biodegradability of the nanocomposite foams, though no biodegradability test was carried out.

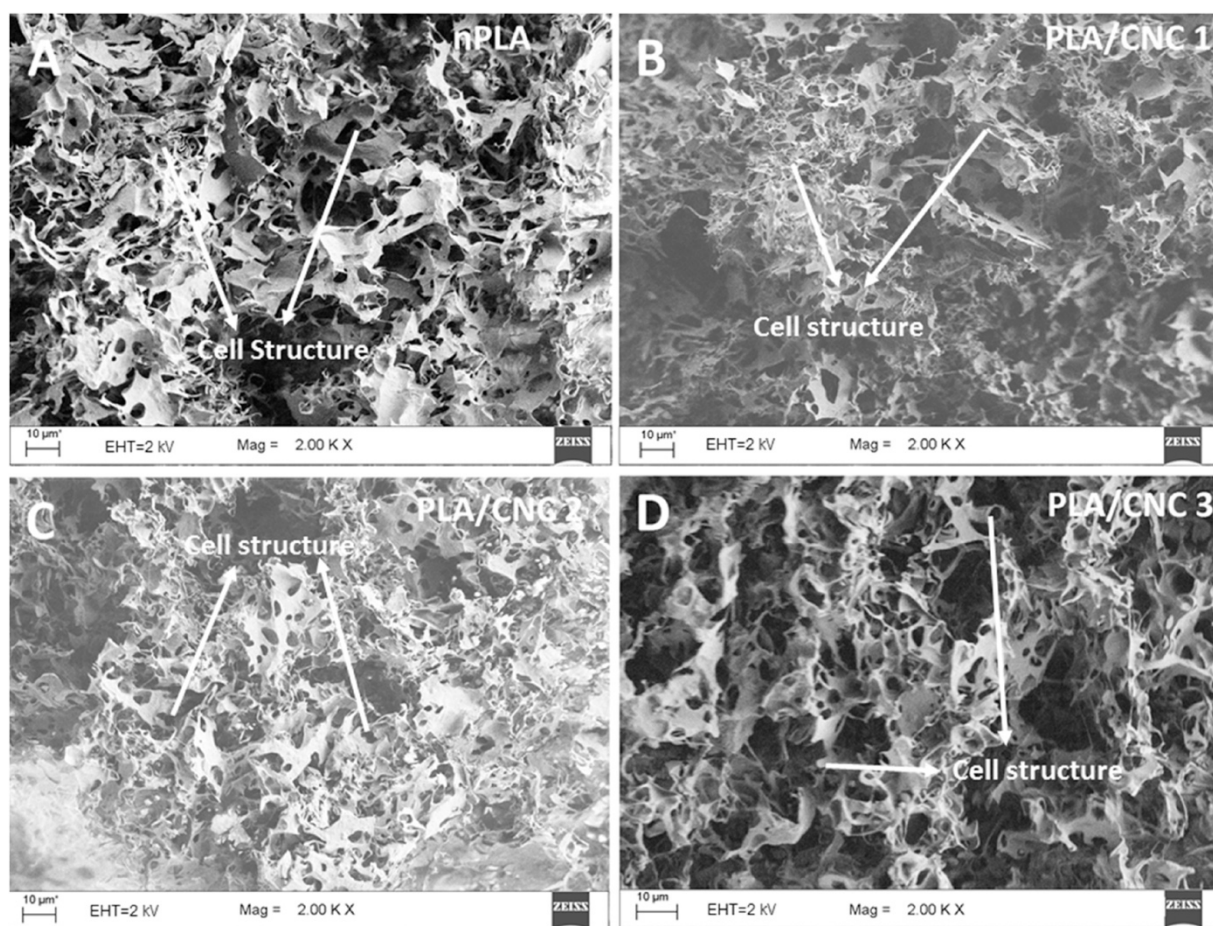


Figure 19: FESEM images of the surface of PLA and PLA/CNC-based foams. Legend: nPLA: neat polylactic acid foam; PLA/CNC X: foam containing cellulose nanocrystals (X indicates the nanofiller wt.% loading). Reprinted with permission from reference 20. Copyright (2018), Elsevier.

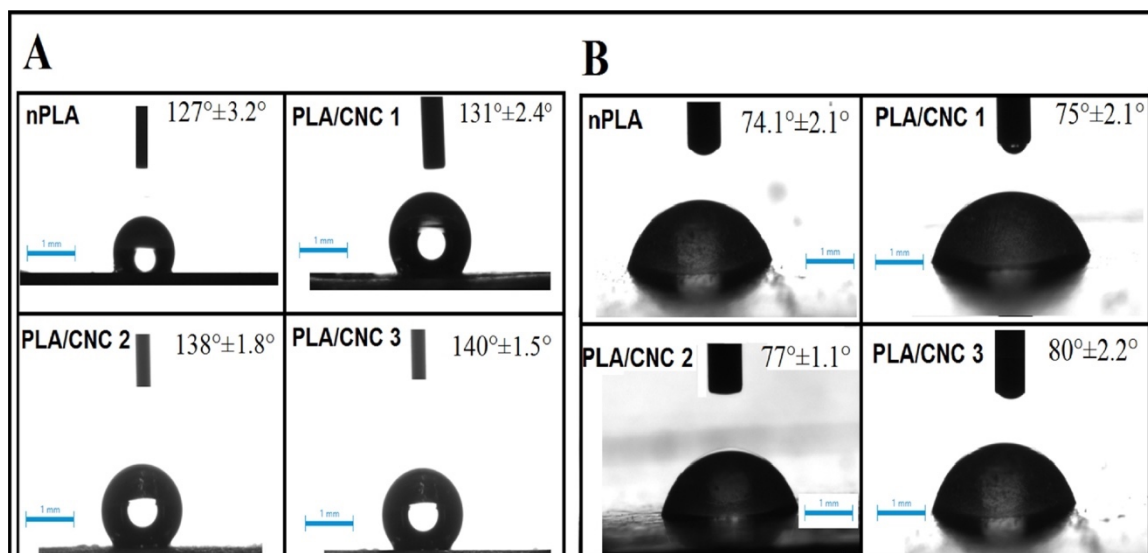
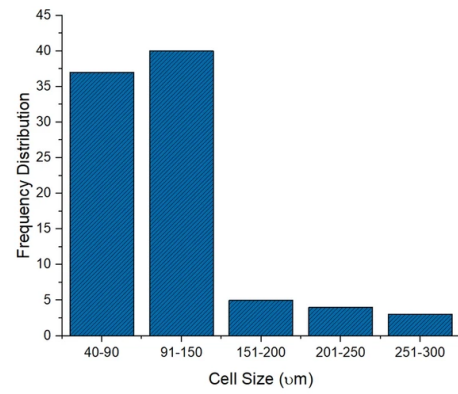
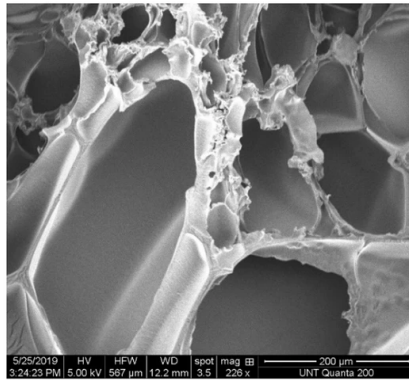
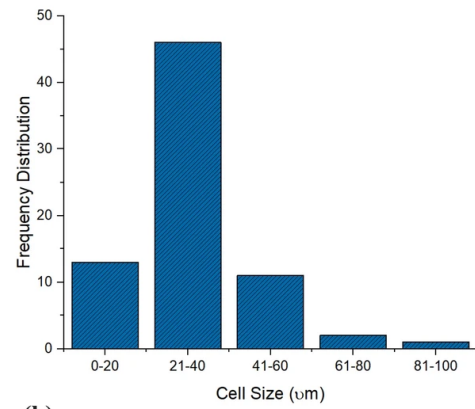
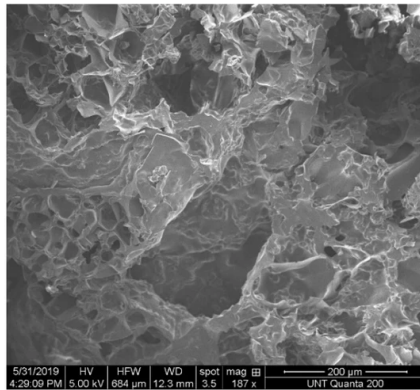


Figure 20: Static contact angle values with water of PLA and PLA/CNC based foams: A: surface with texture, B: surface without texture (compressed surface). Legend: nPLA: neat polylactic acid foam; PLA/CNC X: foam containing cellulose nanocrystals (X indicates the nanofiller wt.% loading Reprinted with permission from reference 20. Copyright (2018), Elsevier.

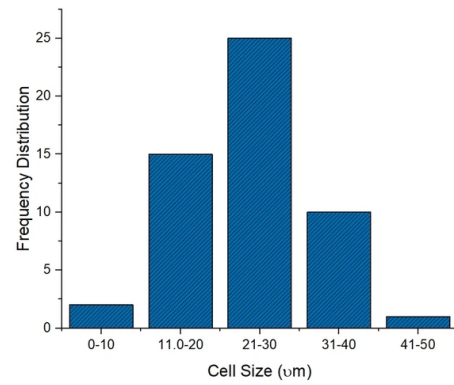
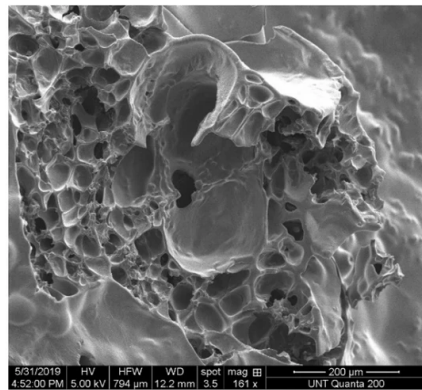
Recently, Oluwabunmi and co-workers²¹ prepared polylactic acid foams containing different loadings of micro cellulose fibrils (i.e., 1.5, 2.25, and 3 wt.%); the foaming process was carried out by means of a solid-state batch process, using carbon dioxide as the blowing agent. The incorporation of the micro cellulose fibrils determined a decrease in the glass transition temperature of the polymer matrix, due to a plasticization effect exerted by the filler. Besides, the cell density of the obtained foams increased with increasing the filler loading; conversely, the cell size decreased (Figure 21). As revealed by biodegradation tests carried out in accordance with the ASTM D 5388-15 standard, the incorporation of increasing amounts of micro cellulose fibrils into the foam enhanced the compostability of the material (Figure 22): 79.4% mineralization was recorded for the foam embedding 3 wt.% of filler after 50 days of incubation, with around 13.4% increase in mineralization compared to the unfilled polylactic acid foam.



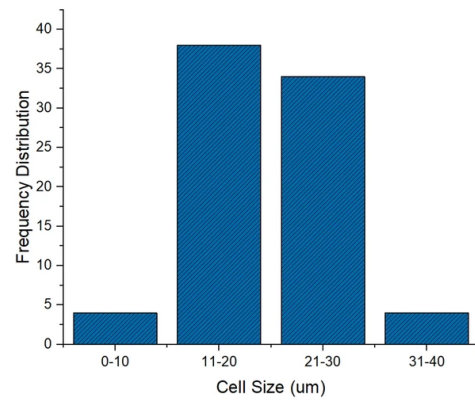
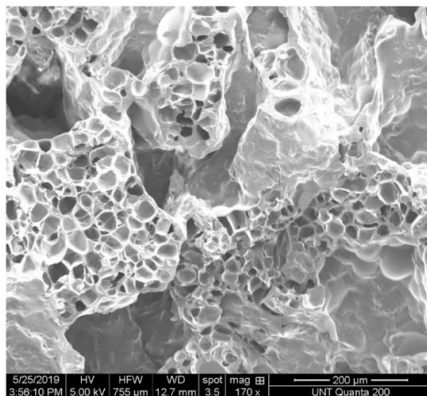
(a)



(b)



(c)



(d)

Figure 21: SEM micrographs and cell size vs. frequency distribution for the investigated foams. Legend: PLA_0f: neat polylactic acid foam; PLA_Af: foam containing 1.5 wt.% of micro cellulose fibrils; PLA_Bf: foam containing 2.25 wt.% of micro cellulose fibrils; PLA_Cf: foam containing 3 wt.% of micro cellulose fibrils. Reprinted from reference 21 under CC BY license.

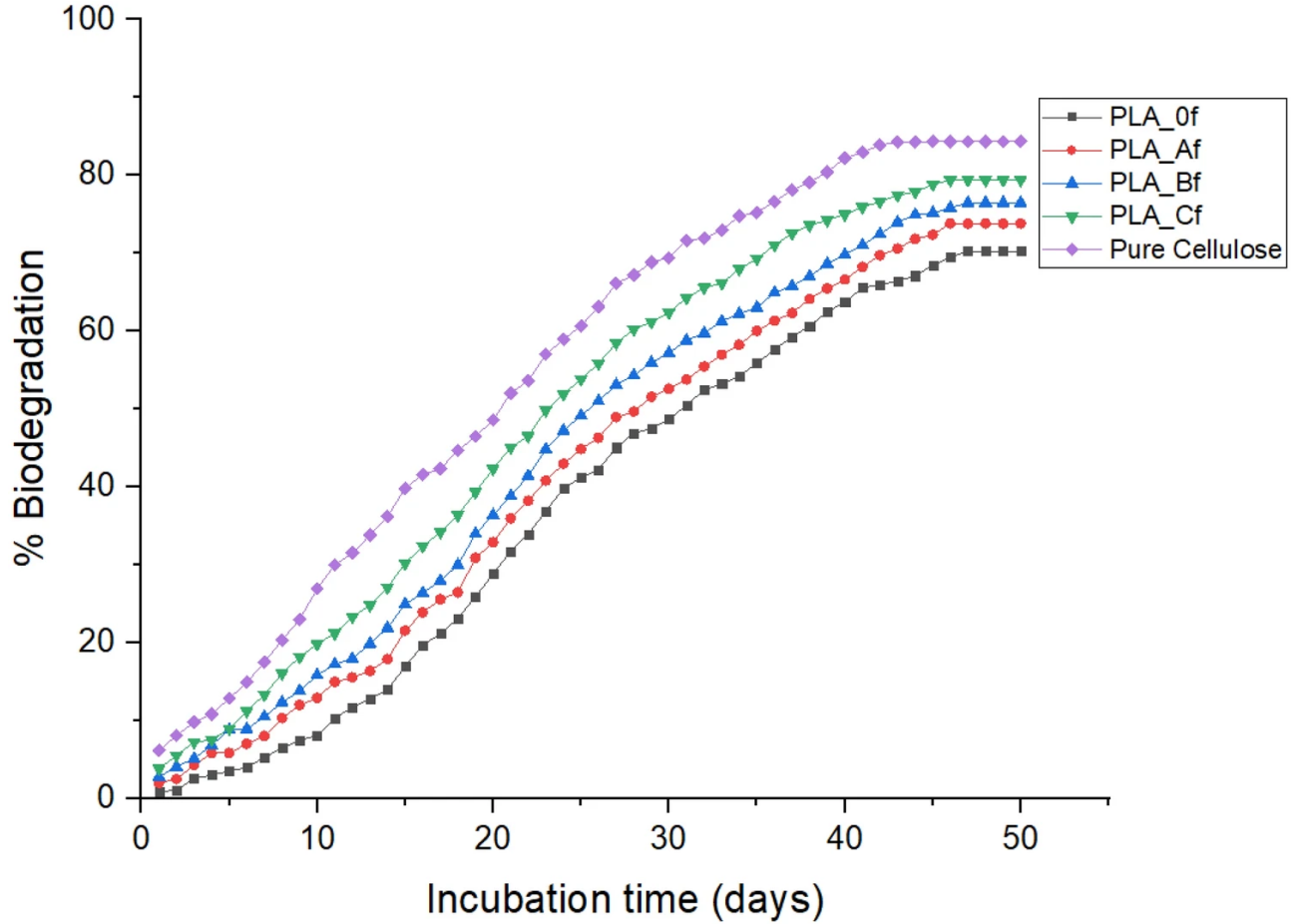


Figure 22: Percentage of biodegradation for the investigated foams. Legend: PLA_0f: neat polylactic acid foam; PLA_Af: foam containing 1.5 wt.% of micro cellulose fibrils; PLA_Bf: foam containing 2.25 wt.% of micro cellulose fibrils; PLA_Cf: foam containing 3 wt.% of micro cellulose fibrils; pure cellulose: micro cellulose fibrils. Reprinted from reference 21 under CC BY license.

The effect of the incorporation of multi-walled carbon nanotubes in a polylactic acid foam on the rheological and thermal behavior, as well as on the material's foamability was recently investigated by Li and co-workers²², who prepared super-high volume expansion ratio nanocomposite materials, using supercritical carbon dioxide as the blowing agent. In particular, the morphology and the overall behavior of the unfilled foam were compared with those of the filled counterparts, using four different nanofiller loadings (i.e., 0.5, 1, 2, and 3 wt.%). Before the foaming process, the presence of the nanofiller, regardless of its loading, did not affect the glass transition temperature (T_g) of the polymer matrix. Conversely, the blowing agent (CO_2) was responsible for a significant decrease of T_g (by about 20°C), as it exerted a plasticization effect on the obtained nanostructured foams. Besides, as assessed by SEM analyses (Figure 23), the incorporation of the nanofiller was found to enhance the pore morphology (regularity) and to decrease the pore size (from about 113.5 to 83.5 μm , for the unfilled polylactic acid foam and the nanocomposite foam incorporating the highest filler loading, respectively): this finding was attributed to the reinforcing effect provided by the multi-walled carbon nanotubes, limiting the pore growth in the molten polymer during the foaming process. Finally, the authors claimed the biodegradability of the nanocomposite foams, though no biodegradability test was carried out.

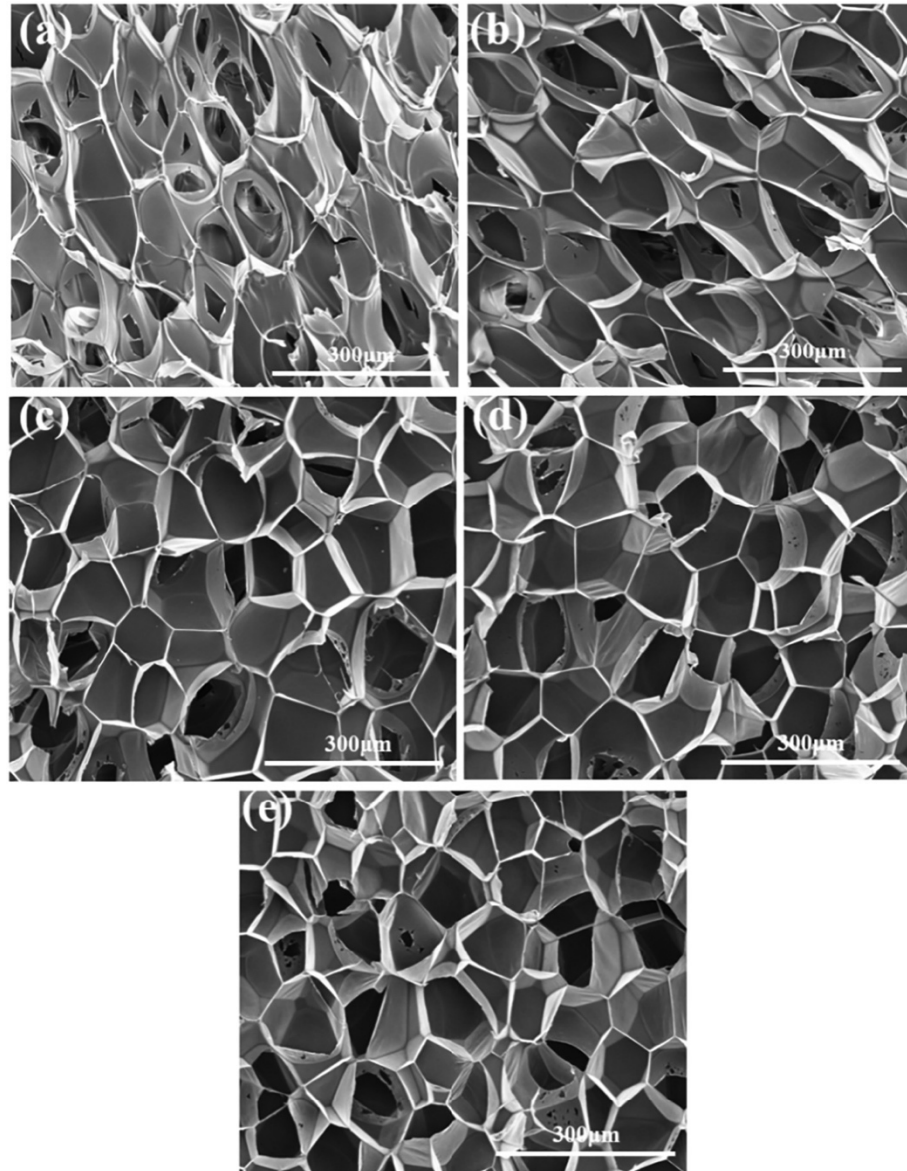


Figure 23: Microcellular morphology of diverse PLA foams prepared at 115°C: (a) pure PLA foam, (b) PLA foam containing 0.5 wt.% of multi-walled carbon nanotubes, (c) PLA foam containing 1 wt.% of multi-walled carbon nanotubes, (d) PLA foam containing 2 wt.% of multi-walled carbon nanotubes, (e) PLA foam containing 3 wt.% of multi-walled carbon nanotubes. Reprinted with permission from reference 22. Copyright (2020), Elsevier.

Progresses in starch-based biodegradable foams

The most recent advances concerning the development of starch-based biodegradable foams assess the suitability of starch, recovered from different natural sources, for different applications. As an example, Cruz-Tirado and co-workers²³ isolated this polysaccharide from three Andean-native crops, namely sweet potato (*Ipomoea batatas*), arracacha (*Arracacia xanthorrhiza*), and oca (*Oxalis tuberosa*). The suitability of the recovered starches to produce foamed trays by thermopressing was assessed. In particular, the obtained trays (Figure 24) exhibited satisfactory expansion and low density as well; conversely, due to the high polarity of the starches, the trays showed high water sorption (beyond 50%) and low mechanical features, with limited differences among the different types of fomed starch. Again, it is worth noting that the biodegradability of the trays was claimed, though no biodegradability test was carried out.

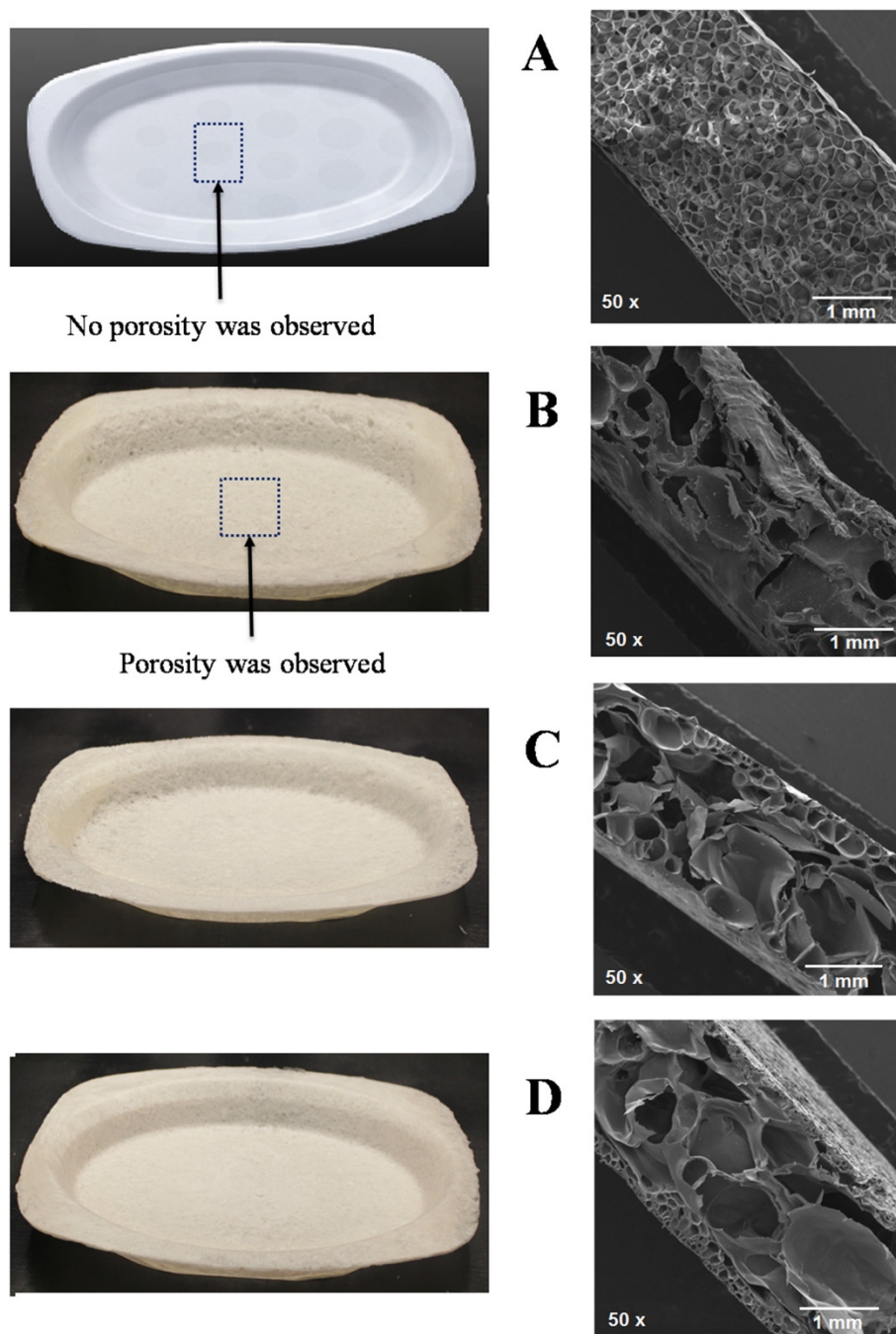


Figure 24: Foam tray color and microstructure: A) Expanded polystyrene used as reference, B) arracacha starch foam tray, C) sweet potato starch foam tray, and D) oca starch foam tray. Reprinted with permission from reference 23. Copyright (2010), Elsevier.

Another recent example come from Engel and co-workers ²⁴, who assessed the biodegradability and potential utilization of thermoplastic cassava starch-based foams prepared by means of thermal expansion and incorporated with Cabernet Sauvignon grape stalks, suitable for packaging low moisture content foods (such as English cake). The obtained foams exhibited higher bulk and true densities and porosities with respect to expanded polystyrene, utilized as a reference (Table 5); besides, the overall mechanical behavior was acceptable for the envisaged application. Finally, the results from biodegradability tests (using a soil burial method) demonstrated the complete biodegradation of the foams (with or without grape stalks) after 7 weeks (Figure 25).

Table 5: Bulk density, true density, and porosity of cassava starch-based foams and of commercial expanded polystyrene

Foam sample	Bulk density (g/cm³)	True density (g/cm³)	Porosity (%)
Commercial expanded polystyrene (reference)	0.031	0.077	60
Cassava starch	0.21	1.279	84
Cassava starch + grape stalks	0.18	1.447	87

The effect of the incorporation of spent coffee ground (at 10 wt.%) and oregano essential oil (at different loadings, namely: 4, 6, 8, and 10 wt.%) on the antibacterial properties, water resistance, and mechanical behavior of cassava starch foams obtained by compression molding was thoroughly investigated by Trongchuen and co-workers. ²⁶ The combination of spent coffee ground and essential oil (at 8 wt.%) was fully effective in inhibiting the growth of *E. coli* and *S. aureus*; besides, the presence of the essential oil decreased the polarity of the foams, hence increasing the water resistance. Conversely, both flexural strength and biodegradability were negatively affected by the incorporation of increasing amounts of essential oil.



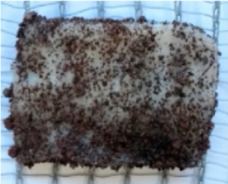

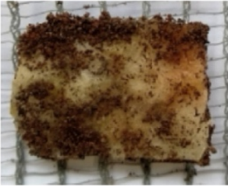
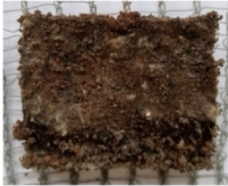







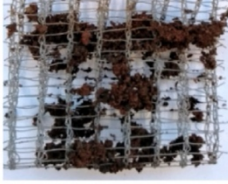


Week	Cassava starch	Cassava starch/grape stalks
0		
1		
2		
3		
4		
5		
6		
7		

Figure 25: Biodegradability test images of cassava starch-based foams, and cassava starch-based foams incorporated with grape stalks at different times of soil burial. Reprinted from reference 24 under CC BY license.

Progresses in polyvinyl alcohol-based biodegradable foams

The current literature provides some interesting examples concerning the design and application of new biodegradable polyvinyl alcohol (PVA)-based foams. Some of the most recent advances will be summarized in the next paragraphs.

Yin and co-workers²⁶ exploited a two-step foaming process for producing polyvinyl alcohol microcellular foams, employing supercritical CO₂ as the foaming agent and ethylene glycol at different loadings (namely, 10, 20, 30, 40, and 50 phr) as a plasticizer. The incorporation of increasing amounts of the plasticizer accounted for the decrease of the melting point of the polyvinyl alcohol, as well as for the widening of its processing window. Further, ethylene glycol was responsible for a significant decrease in the melt strength of the polymer, reducing the inter-/intra-hydrogen bonding interactions in PVA, hence favoring the diffusion of the blowing agent and the subsequent foaming process. As far as the morphology of the foams is concerned, the presence of increasing amounts of plasticizer remarkably improved the number of formed cells and their average size (that achieved 12.75 μm in the presence of 30 phr of ethylene glycol, compared to 6.85 μm of the neat polyvinyl alcohol foam), enhancing, at the same time, their uniformity of distribution.

Wang and co-workers²⁷ combined a thermal process in a single-screw extruder with supercritical CO₂ foaming for producing biodegradable polyvinyl alcohol bead foams, using glycerol or water as plasticizers, and performing the welding of the beads during the foaming process in suitable molds. The foaming process (schematized in Figure 26) was thoroughly investigated, evaluating the effect of the plasticizer (both type and loading), of the foaming temperature, and of the filling content of PVA beads in the foaming mold.

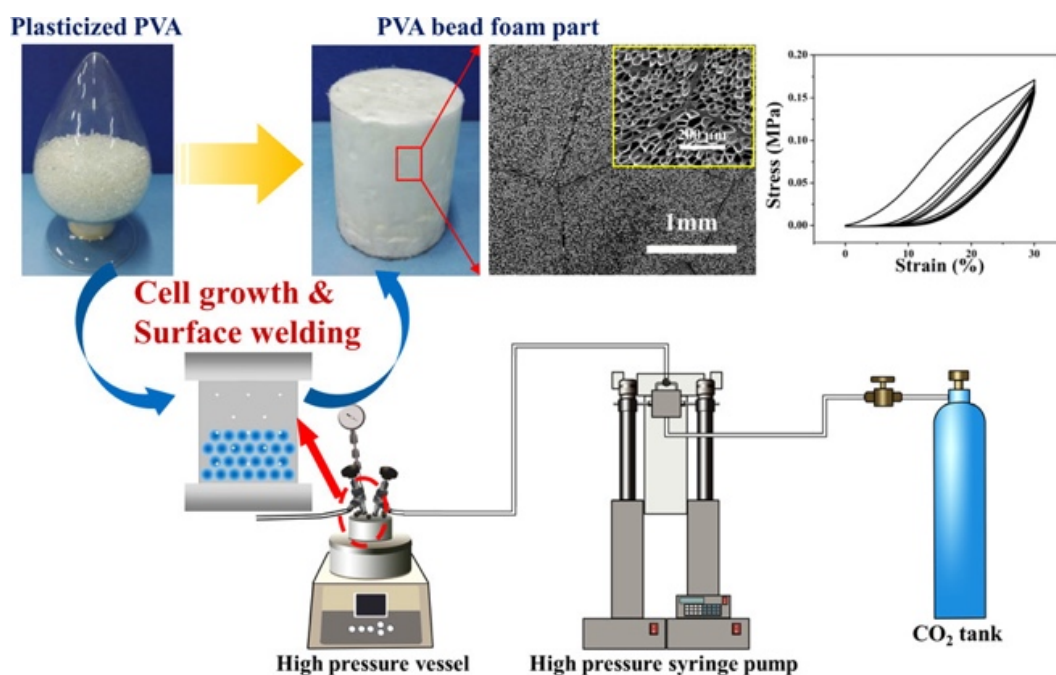


Figure 26: Schematic illustration of the fabrication process of PVA bead foaming parts. Reprinted with permission from reference 27. Copyright (2021), American Chemical Society.

Both water (Figure 27) and glycerol (Figure 28) were very effective in plasticizing the polymer matrix and favoring the formation of regular cells, homogeneously distributed. Besides, the foaming temperature was found to significantly impact the cellular structure: as shown in Figure 29, increasing the foaming temperature resulted in an increased average size of the cells.

Finally, the obtained foams exhibited high compressive strength and good resilience during cyclic compression tests, suggesting their potential as an alternative to conventional fossil-derived polymeric systems for packaging. Again, it is worth noticing that the biodegradability of the foamed parts was claimed, though no biodegradability test was carried out.

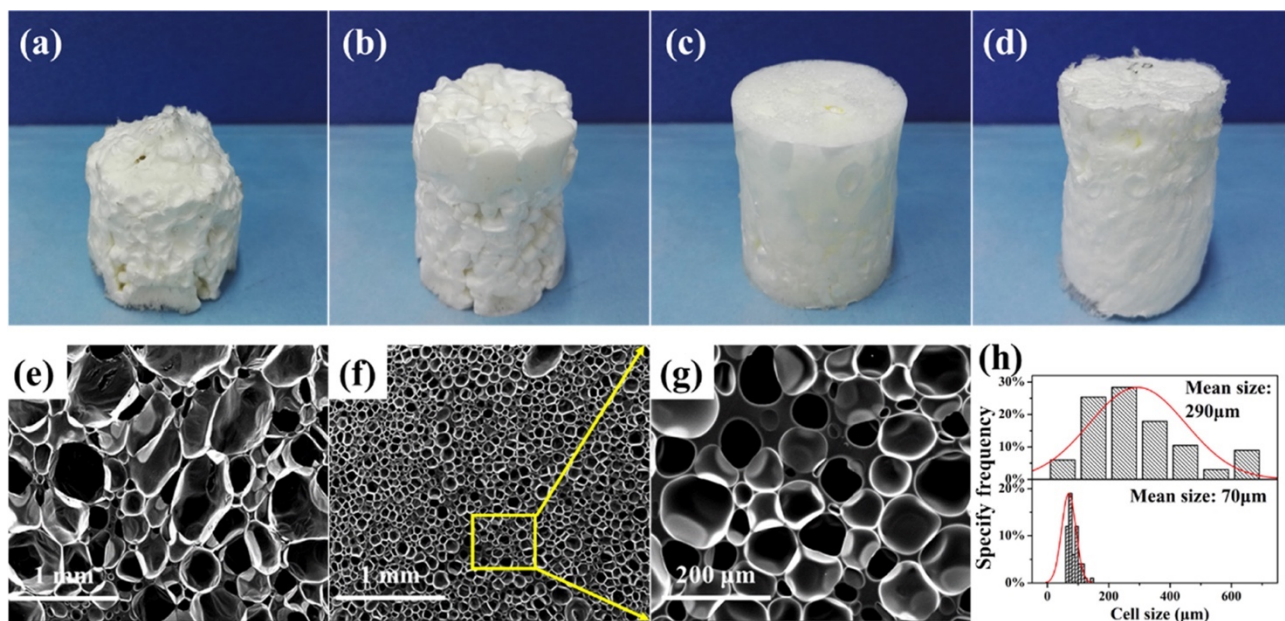


Figure 27: Digital photos showing the foam parts prepared from water-plasticized PVA beads with different filling contents in the foaming mold: 5% (a), 10% (b), 15% (c), and 20% (d). SEM images showing the cellular structure of foamed parts with the filling content of PVA beads in the foaming mold of 15% (e) and 25% (f, g); cell size distribution of foamed parts with the filling content of PVA beads in the foaming mold of 15% (h, up) and 25% (h, down). Reprinted with permission from reference 27. Copyright (2021), American Chemical Society.

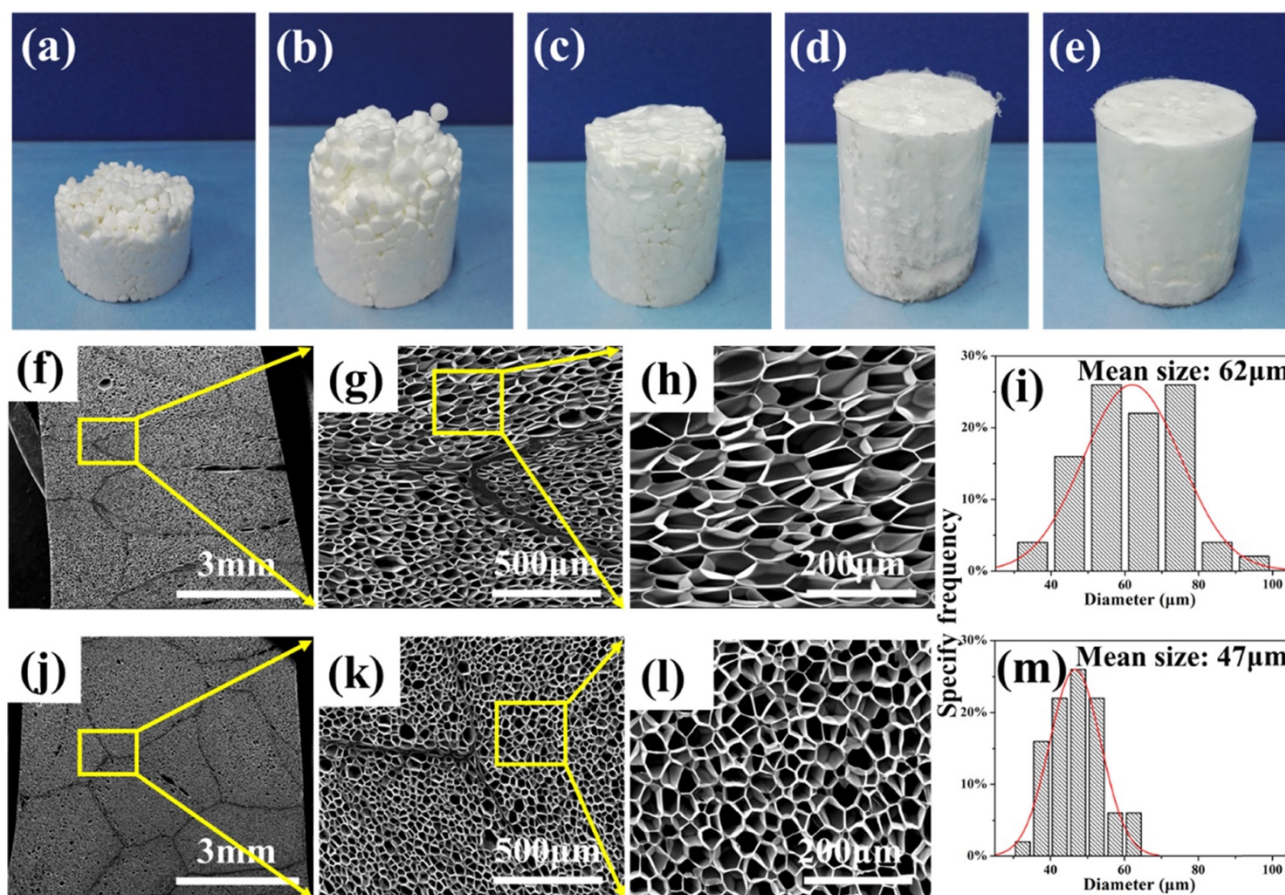


Figure 28: Digital photos showing the foam parts prepared from glycerol-plasticized PVA beads with different filling contents in the foaming mold: 5% (a), 10% (b), 15% (c), 20% (d), and 25% (e). SEM images showing the cellular structure of foamed parts with 20% (f–h) and 25% (j–l) PVA beads (filling content in the foaming mold); cell size distribution of foamed parts with 20% (i) and 25% (m) PVA beads (filling content in the foaming mold). Reprinted with permission from reference 27. Copyright (2021), American Chemical Society.

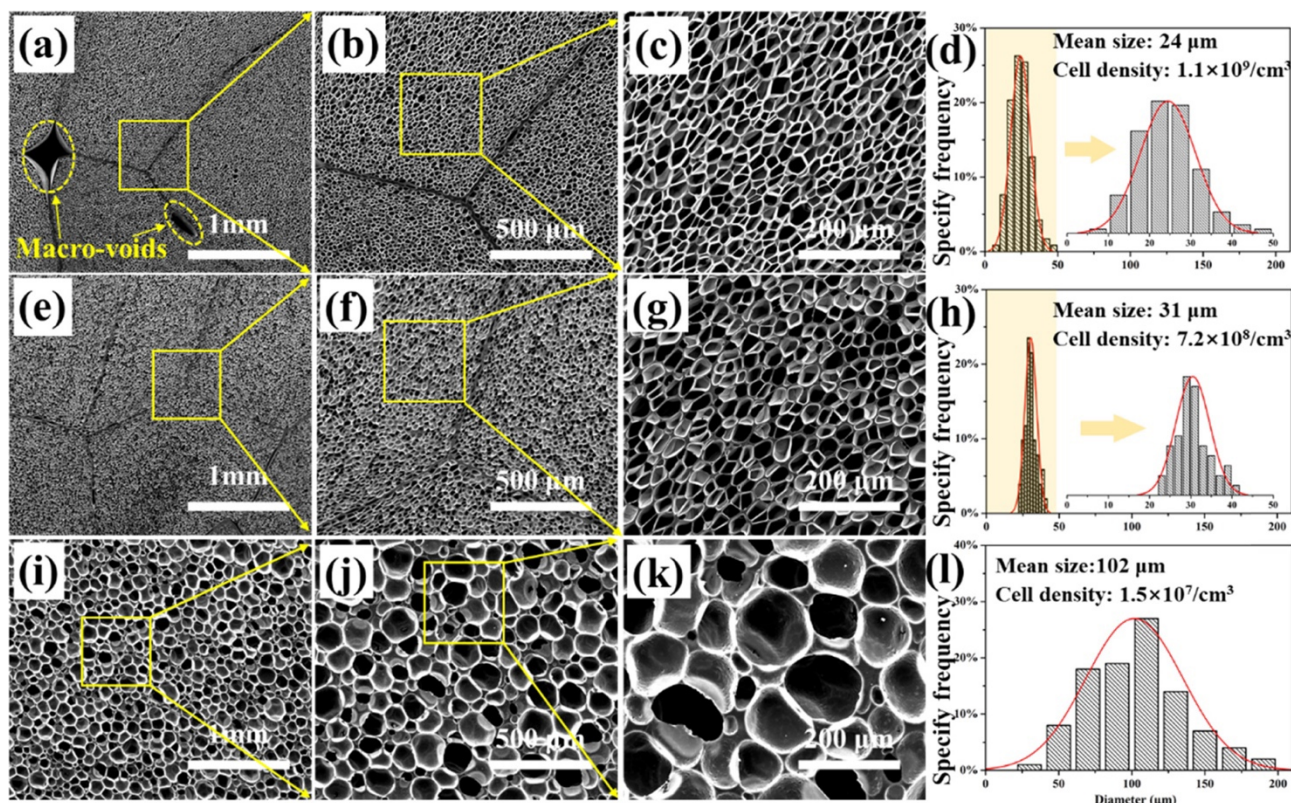
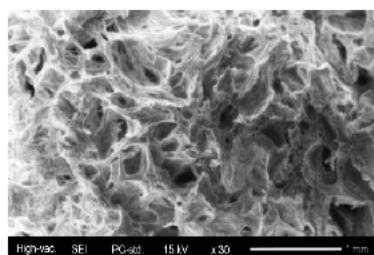
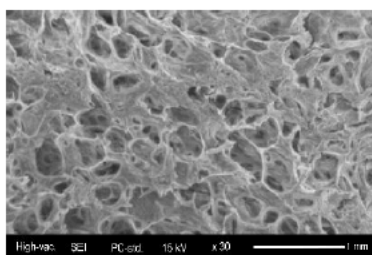


Figure 29: SEM images showing the cellular structure of bead foam parts with 25% filling content (in the foaming mold) foamed at different temperatures, namely: 165 °C (a–c), 175 °C (e–g), and 185 °C (i–k); cell size distribution, mean size, and cell density of foam parts foamed at 165 °C (d), 175 °C (h), and 185 °C (l). Reprinted with permission from reference 27. Copyright (2021), American Chemical Society.

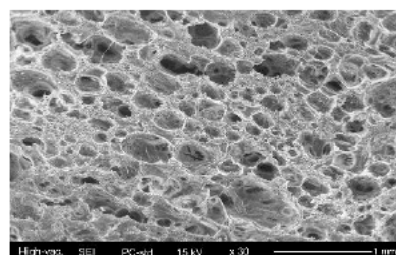
Very recently, Liu and co-workers²⁸ prepared and characterized foamed composites, suitable for cushion packaging applications, made of polyvinyl alcohol and bagasse fibers; water was employed as a plasticizer, CaCO₃ as a nucleating agent, and sodium tetraborate as a cross-linker. First, good compatibility between the two components of the foamed composites was observed, without any agglomeration of the fibers on the surface of the composites; besides, by increasing the PVA content, a more regular formation of open cells occurred, as shown in Figure 30, with an increased number of cells with a gradually decreased size and increased cell wall thickness. Finally, the mechanical behavior (in terms of yield strength, stiffness, and static cushioning) of the obtained foamed composites was similar to that of a high-density commercial expanded polystyrene, chosen as reference material for the envisaged application.



(a) PVA content of 8.41 wt%



(b) PVA content of 9.67 wt%



(c) PVA content of 10.91 wt%

Figure 30: SEM morphologies of internal sections of the foamed composites at different PVA loadings. Reprinted from reference 28 under CC BY license.

Conclusion

The significant developments so far achieved in the design, formulation, and production of biodegradable foams are very promising and seem to pave the way toward a greener world. In fact, the availability of natural sources, the possibility of their easy recovery/isolation, as well as the setup of foaming technologies with low environmental impact make biodegradable foams suitable for even industrial applications. Despite these advantages, some issues are still challenging and will have to be considered in the next future. First, the biodegradable foams may incorporate additives, dyes, and other chemical products that could be leached out during the biodegradation steps, hence contaminating the soil and the groundwater, with a significant impact on the surrounding environment. Then, some of the raw materials employed for producing biodegradable foams are still not cost-effective for a direct industrial exploitation: therefore, further research efforts are needed for implementing the recovery and use of these materials at a large scale and keeping adequate costs. Finally, success in the use of biodegradable foams for new market uses will be achieved only when it will be possible to set up clear disposal plans, design effective large-scale processes and equipment, identify suitable, standardized, and reliable methods for evaluating the overall features of the foamed materials (also considering a circular economy approach), and educate people on how to manage the end-of-life of these products. It is expected, in the forthcoming years, to identify new advanced technological processes, material sources, and therefore new potential markets for biodegradable foams, hence helping to reduce the dependence on fossil resources.

References

- (1) Gautam, R.; Bassi, A.S.; Yanful, E.K. A Review of Biodegradation of Synthetic Plastic and Foams. *Appl. Biochem. Biotechnol.* **2007**, *141*, 85-108. <https://doi.org/10.1007/s12010-007-9212-6>
- (2) ASTM D 6400-21 "Standard Specification for Labeling of Plastics Designed to be Aerobically Composted in Municipal or Industrial Facilities"
- (3) Kyrikou, J.; Briassoulis, D. Biodegradation of Agricultural Plastic Films: A Critical Review. *J. Polym. Environ.* **2007**, *15*, 125-150. <https://doi.org/10.1007/s10924-007-0053-8>
- (4) Grima, S.; Bellon-Maurel, V.; Feuilloley, P.; Silvestre, F. Aerobic Biodegradation of Polymers in Solid-State Conditions: A Review of Environmental and Physicochemical Parameter Settings in Laboratory Simulation. *J. Polymer Environ.* **2002**, *8*, 183-195. <https://doi.org/10.1023/A:1015297727244>
- (5) Swift, G. Requirements for biodegradable water-soluble polymers. *Polym. Degrad. Stabil.* **1998**, *59*, 19-24. [https://doi.org/10.1016/S0141-3910\(97\)00162-6](https://doi.org/10.1016/S0141-3910(97)00162-6)
- (6) Acemoglu, M. Chemistry of polymer biodegradation and implications on parenteral drug delivery. *Int. J. Pharm.* **2004**, *277*, 133-139. <https://doi.org/10.1016/j.ijpharm.2003.06.002>
- (7) Anderson, J.M.; Shive, M.S. Biodegradation and biocompatibility of PLA and PLGA microspheres. *Adv. Drug Deliv. Rev.* **2012**, *64*, 72-82. <https://doi.org/10.1016/j.addr.2012.09.004>
- (8) Ramesh, N.S.; Malwitz, Nelson. Extrusion of novel water soluble biodegradable foams. Annual Technical Conference - ANTEC, Conference Proceedings **1995**, *2*, 2171-2177.
- (9) Zobel, H.F. Molecules to Granules: A Comprehensive Starch Review. *Starch – Stärke* **1988**, *40* (2), 44-50. <https://doi.org/10.1002/star.19880400203>
- (10) Shogren, R.L.; Lawton, J.W.; Doane, W.M.; Tiefenbacher, K.F. Structure and morphology of baked starch foams. *Polymer* **1998**, *39* (25), 6649-6655. [https://doi.org/10.1016/S0032-3861\(97\)10303-2](https://doi.org/10.1016/S0032-3861(97)10303-2)
- (11) Yu, Z.; Xiao, Y.; Tian, H.; Liu, S.; Zeng, J.; Luo, X. Bagasse as functional fillers to improve and control biodegradability of soy oil-based rigid polyurethane foams. *Korean J. Chem. Eng.* **2019**, *36* (10), 1740-1745. <https://doi.org/10.1007/s11814-019-0349-0>
- (12) Paciork-Sadowska, J.; Borowicz, M.; Chmiel, E.; Lubczak, J. Use of a Mixture of Polyols Based on Metasilicic Acid and Recycled PLA for Synthesis of Rigid Polyurethane Foams Susceptible to Biodegradation. *Int. J. Mol. Sci.* **2021**, *22*, 69. <https://doi.org/10.3390/ijms22010069>
- (13) Fang, Z.; Qiu, C.; Ji, D.; Yang, Z.; Zhu, N.; Meng, J.; Hu, X.; Guo, K. Development of High-Performance Biodegradable Rigid Polyurethane Foams Using Full Modified Soy-Based Polyols. *J. Agric. Food Chem.* **2019**, *67*, 2220-2226. <https://doi.org/10.1021/acs.jafc.8b05342>
- (14) Luo, X.; Xiao, Y.; Wu, Q.; Zeng, J. Development of high-performance biodegradable rigid polyurethane foams using all bioresource-based polyols: Lignin and soy oil-derived polyols. *Int. J. Biol. Macromol.* **2018**, *115*, 786-791. <https://doi.org/10.1016/j.ijbiomac.2018.04.126>

- (15) Danjaji, I.D.; Nawang, R.; Ishiaku, U.S.; Ismail, H.; Mohd Ishak, Z.A.M. Degradation studies and moisture uptake of sago-starch-filled linear low-density polyethylene composites. *Polym. Test.* **2002**, *21* (1), 75–81. [https://doi.org/10.1016/S0142-9418\(01\)00051-4](https://doi.org/10.1016/S0142-9418(01)00051-4)
- (16) Borowicz, M.; Paciorek-Sadowska, J.; Lubczak, J.; Czuprynski, B. Biodegradable, Flame-Retardant, and Bio-Based Rigid Polyurethane/Polyisocyanurate Foams for Thermal Insulation Application. *Polymers* **2019**, *11*, 1816. doi:10.3390/polym11111816
- (17) Klotz, M.G.; Bryant, D.A.; Hanson, T.E. The microbial sulfur cycle. *Front. Microbiol.* **2011**, *2*, 241. <https://doi.org/10.3389/fmicb.2011.00241>
- (18) Mukherjee, M.; Gurusamy-Thangavelu, S.A.; Kumar Chelike, D.; Alagumalai, A.; Das, B.N.; Jaisankar, S.N.; Baran Mandal, A. Biodegradable polyurethane foam as shoe insole to reduce footwear waste: Optimization by morphological physicochemical and mechanical properties. *Appl. Surf. Sci.* **2020**, *499*, 143966. <https://doi.org/10.1016/j.apsusc.2019.143966>
- (19) Li, B.; Zhao, G.; Wang, G.; Zhang, L.; Gong, J.; Shi, Z. Biodegradable PLA/PBS open-cell foam fabricated by supercritical CO₂ foaming for selective oil-adsorption. *Sep. Purif. Technol.* **2021**, *257*, 117949. <https://doi.org/10.1016/j.seppur.2020.117949>
- (20) Sekhar Borkotoky, S.; Dhar, P.; Katiyar, V. Biodegradable poly (lactic acid)/Cellulose nanocrystals (CNCs) composite microcellular foam: Effect of nanofillers on foam cellular morphology, thermal and wettability behavior. *Int. J. Biol. Macromol.* **2018**, *106*, 433–446. <https://doi.org/10.1016/j.ijbiomac.2017.08.036>
- (21) Oluwabunmi, K.; D'Souza, N.A. Zhao, W.; Choi, T.Y.; Theyson, T. Compostable, fully biobased foams using PLA and micro cellulose for zero energy buildings. *Sci. Rep.* **2020**, *10*, 17771 <https://doi.org/10.1038/s41598-020-74478-y>
- (22) Li, Y.; Yin, D.; Liu, W.; Zhou, H.; Zhang, Y.; Wang, X. Fabrication of biodegradable poly (lactic acid)/carbon nanotube nanocomposite foams: Significant improvement on rheological property and foamability. *Int. J. Biol. Macromol.* **2020**, *163*, 1175–1186. <https://doi.org/10.1016/j.ijbiomac.2020.07.094>
- (23) Cruz-Tirado, J.P.; Vejarano, R.; Tapia-Blácido, D.R.; Barraza-Jáuregui, G.; Siche, R. Biodegradable foam tray based on starches isolated from different Peruvian species. *Int. J. Biol. Macromol.* **2019**, *125*, 800–807. <https://doi.org/10.1016/j.ijbiomac.2018.12.111>
- (24) Engel, J.B.; Ambrosi, A.; Tessaro, I.C. Development of biodegradable starch-based foams incorporated with grape stalks for food packaging. *Carbohydr. Polym.* **2019**, *225*, 115234. <https://doi.org/10.1016/j.carbpol.2019.115234>
- (25) Trongchuen, K.; Ounkaew, A.; Kasemsiri, P.; Hizioglu, S.; Mongkolthanaruk, W.; Wannasutta, R.; Pongsa, U.; Chindaprasirt, P. Bioactive Starch Foam Composite Enriched With Natural Antioxidants from Spent Coffee Ground and Essential Oil. *Starch - Stärke* **2018**, *70*, 1700238. <https://doi.org/10.1002/star.201700238>
- (26) Yin, D.; Xiang, A.; Li, Y.; Qi, H.; Tian, H.; Fan, G. Effect of Plasticizer on the Morphology and Foaming Properties of Poly(vinyl alcohol) Foams by Supercritical CO₂ Foaming Agents. *J. Polym. Environ.* **2019**, *27*, 2878–2885. <https://doi.org/10.1007/s10924-019-01570-4>
- (27) Wang, Q.; Yang, J.; Liu, P.; Li, L. Facile One-Step Approach to Manufacture Environmentally Friendly Poly(vinyl alcohol) Bead Foam Products. *Ind. Eng. Chem. Res.* **2021**, *60*, 2962–2970. <https://dx.doi.org/10.1021/acs.iecr.1c00203>
- (28) Liu, B.; Huang, X.; Wang, S.; Wang, D.; Guo, H. Performance of Polyvinyl Alcohol/Bagasse Fibre Foamed Composites as Cushion Packaging Materials. *Coatings* **2021**, *11*, 1094. <https://doi.org/10.3390/coatings11091094>